MERCURY REMOVAL FROM SIMULATED COAL-FIRED POWER PLANT FLUE GAS USING UV IRRADIATION AND SILICA-TITANIA COMPOSITES

By

ALEXANDER F GRUSS

A DISSERTATION PRESENTED TO THE GRADUATE SCHOOL
OF THE UNIVERSITY OF FLORIDA IN PARTIAL FULFILLMENT
OF THE REQUIREMENTS FOR THE DEGREE OF
DOCTOR OF PHILOSOPHY

UNIVERSITY OF FLORIDA

2011

To everyone who has helped me along the way

ACKNOWLEDGMENTS

I would like to thank my parents, who have always been there for me. Whenever times get tough, I can count on their advice and support to help me get through any situation. I thank my sister for her friendship throughout the years. A special thank you to Amy Borello for making me laugh every day, and for her support in everything I do. Without her this would have been a much different experience.

I would also like to thank Dr. Mazyck for giving me the opportunity to work in his lab and experience small-business technology commercialization. I have learned tremendous lessons that I will take with me throughout my business life. I thank my supervisory committee Dr. Amelia Dempere, Dr. Paul Chadik, and Dr. Chang-Yu Wu for their guidance and suggestions.

I am grateful for the advice, assistance and company of Rick Loftis and Dave Baun, who made working in the lab a more pleasant experience. Thanks go to Anna Casasús for her guidance and help.

I thank the membersof my research group, past and present for their support, especially Amy Borello, Heather Byrne, William Kostedt IV, and Jennifer Stokke.

TABLE OF CONTENTS

page

ACKNOWLEDGMENTS 4

LIST OF TABLES 7

LIST OF FIGURES 8

ABSTRACT 11

CHAPTER

1 INTRODUCTION 12

2 LITERATURE REVIEW 16

Photocatalysis 16
Methods of Mercury Removal 17
Silica-Titania Composites 19
Mercury Oxidation 21

3 EXPERIMENTAL 23

STCP Production 23
Characterization 23
Experimental Setup 24
Oxidation Studies 25
Flue Gas Simulation 26
Mercury Analysis 27

4 MERCURY OXIDATION BY UV 30

Effect of Contact Time 30
Effect of Water Vapor and Temperature 31
Effect of UV 33
Effect of Ozone 33
Summary 34

5 MERCURY VAPOR REMOVAL FROM BENCH-SCALE SIMULATED FLUE-GAS USING STCP 39

Baseline Experiments 40
Effect of NO_2 40
Effect of SO_2 41
Effect of HCl 41

Effect of Simulated Flue Gas 42
Summary 43

6 PILOT-SCALE MERCURY REMOVAL USING STCP 48

Materials and Methods 50
STCP Material Development 50
Evaluation of Mercury Removal 52
Scaled-Up Evaluation of Mercury Removal from Simulated Flue Gas Using STCP 53
Results and Discussion 53
STCP Material Development 53
STCP Material Characterization 55
XRD 55
SEM Imaging 56
Hardness/Durability 56
Pore size, pore volume, and surface area 57
Simulated Flue Gas Bench-scale Experiments 57
4 ACFM Pilot-Scale Data 59
Competitive Analysis 60
Summary 60

7 CONCLUSIONS 69

APPENDIX: VOC REMOVAL BY STC PELLETS 72

Experimental 74
Adsorption 74
Regeneration 75
Results 75
Adsorption Studies 75
Regeneration of STC 76
Summary 77

LIST OF REFERENCES 83

BIOGRAPHICAL SKETCH 92

LIST OF TABLES

Table		page
5-1	Summary of results in % mercury removal.	43
5-2	Standard error of STCP results in % mercury removal.	43
6-1	Coating recipes that were attempted during this study.	61
6-2	Summary of durability test results.	61
6-3	Characteristics of PEG and non-PEG packing.	61
6-4	Competitive analysis of STCP versus two widely accepted commercial technologies for Hg removal from flue gas.	62

LIST OF FIGURES

Figure		page
2-1	Schematic of band gap irradiation of a semiconductor particle	22
3-1	Test stand setup for mercury oxidation study	28
3-2	Test stand setup for STCP study	29
3-3	Hg analysis setup with impingers and Zeeman	29
4-1	Mercury oxidation by 254 nm UV at 300°F and 26,000 ppmv WVC.	35
4-2	Mercury oxidation by 185 nm UV at 300°F and 26,000 ppmv WVC.	35
4-3	Mercury oxidation vs water vapor concentration varying UV wavelength at ca. 80°F.	36
4-4	Mercury oxidation vs water concentration varying UV wavelength at 200º F.	36
4-5	Mercury oxidation vs water concentration varying UV wavelength at 300°F.	37
4-6	Mercury oxidation by ozone vs water concentration at ca. 80°F.	37
4-7	Mercury oxidation by ozone vs water concentration at 200°F.	38
4-8	Mercury oxidation by ozone vs water concentration at 300°F.	38
5-1	Hg oxidation/removal using STCP at 275°F and 43,000 ppm_v WVC.	44
5-2	Hg oxidation/removal using STCP at 275°F and 43,000 ppm_v WVC, 250 ppm_v NO_2	44
5-3	Long-term Hg oxidation/removal using STCP at 275°F and 43,000 ppm_v WVC, 250 ppm_v NO_2.	45
5-4	Hg oxidation/removal using STCP at 275°F and 43,000 ppm_v WVC, 350 ppm_v SO_2.	45
5-5	Hg oxidation/removal using STCP at 275°F and 43,000 ppm_v WVC, 100 ppm_v HCl.	46
5-6	Hg oxidation/removal using STCP at 275°F and 43,000 ppm_v WVC, 100 ppm_v HCl, 350 ppm_v SO_2.	46
5-7	Hg oxidation/removal using STCP at 275°F and 43,000 ppm_v WVC, 250 ppm_v NO_2, 100 ppm_v HCl, 350 ppm_v SO_2.	47

5-8 Hg oxidation/removal using STCP at 375°F and 197,000 ppm_v WVC, 250 ppm_v NO_2, 100 ppm_v HCl, 350 ppm_v SO_2. 47

6-1 Test stand schematic for bench-scale studiesfor evaluation of STCP for Hg removal from simulated flue gas. 62

6-2 Schematic of 4 ACFM pilot-scale reactor used for scaled-up evaluation of STCP for Hg removal from simulated flue gas. 63

6-3 UV transmission through a packed bed of various materials. 63

6-4 SEM imaging of PEG packing (5000X magnification). 64

6-5 SEM imaging of non-PEG packing (5,000X magnification). 64

6-6 SEM imaging of used packing (5,000X magnification). 65

6-7 375˚F, 2 s contact time, 10 ppb Hg, no added humidity, non-PEG STCP. 65

6-8 375˚F, 2 s contact time, 10 ppb Hg, 4% relative humidity, non-PEG STCP, 100 ppm HCl. 66

6-9 375˚F, 2 s contact time, 10 ppb Hg, 4% relative humidity, non-PEG STCP, 100 ppm HCl, 350 ppm SO_2. 66

6-10 375˚F, 2 s contact time, 10 ppb Hg, 4% relative humidity, non-PEG STCP, 100 ppm HCl, 350 ppm SO_2, 250 ppm NO_2. 67

6-11 375˚F, 2 s contact time, 10 ppb Hg, 4% relative humidity, 100 ppm HCl, 350 ppm SO_2, 250 ppm NO_2. Media: 3 mm by 5 mm cylindrical STC pellets (140Å pore size, 12% TiO_2). 67

6-12 375˚F, 1 s contact time, 10 ppb Hg, 4% relative humidity, non-PEG STCP, 100 ppm HCl, 350 ppm SO_2, 250 ppm NO_2. 68

6-13 Results of 4 ACFM pilot-scale evaluation of non-PEG coated honeycomb at the following conditions: 375 or 200˚F, 1.2 s contact time in each of two sections defined earlier, 10 ppb Hg, 4% relative humidity, and 100 ppm HCl. ... 68

A-1 Experimental setup for toluene adsorption. 79

A-2 Experimental setup for ethanol adsorption. 79

A-3 Experimental setup for regeneration. 80

A-4 Toluene adsorption at 72 ft/min face velocity. 80

A-5 Toluene adsorption at 176 ft/min face velocity. 81

A-6 Toluene adsorption by virgin and regenerated STC pellets. Note that the virgin and regenerated pellets remove the same percentage of toluene at the last data point. 81

A-7 Ethanol removal before and after regeneration with sweep air. 82

A-8 Toluene removal after several regenerations with sweep air. 82

Abstract of Dissertation Presented to the Graduate School
of the University of Florida in Partial Fulfillment of the
Requirements for the Degree of Doctor of Philosophy

MERCURY REMOVAL FROM SIMULATED COAL-FIRED POWER PLANT FLUE GAS USING UV IRRADIATION AND SILICA-TITANIA COMPOSITES

By

ALEXANDER F GRUSS

August 2011

Chair:David Mazyck
Major: Environmental Engineering Sciences

Mercury is listed as a hazardous air pollutant (HAP) because of its adverse health effects on humans. Without technologies that effectively remove mercury that is contained in the flue gas of coal combustion power plants, the long-term effects on the nation's health could be catastrophic.

This research builds on previous work to examine mercury removal at typical flue gas temperatures (up to 375°F), multiple flue gas components (SO_2, NO_2, HCl), and short contact times (0.3 - 2 s) by studying photocatalytic oxidation and capture of mercury by a silica-titania composite technology coated onto ceramic packing material. Experiments conducted under flue gas conditions showed little change in Hg removal performance when the temperature was increased from 275°F to 375°F. Both oxidation and adsorption seemed to be inhibited by moisture at 375°F, except when chlorine was present. Moisture had a significant detrimental effect on oxidation levels of mercury by UV alone, particularly at a wavelength of 254 nm.

CHAPTER 1
INTRODUCTION

In 2010, coal combustion accounted for almost half of the electricity supply (45%) in the US and is the predominant source of energy in the world (1). Coal-fired power plants account for over one third of total US anthropogenic mercury emissions, making them the largest single source of mercury air emissions (2). Globally, almost two-thirds of total anthropogenic mercury emissions in 2000 came from combustion of fossil fuels, of which coal combustion had a large share (3). Emission of certain gases from coal combustion power plants, such as nitrogen oxides (NO_x) and sulfur dioxide (SO_2) are regulated by the EPA (4, 5). However, mercury emissions from coal combustion power plants are currently not regulated.

The 1990 Amendments to the Clean Air Act directed the Environmental Protection Agency (EPA) to study the health and environmental impacts of HAPs (6). The EPA found that mercury emitted into the atmosphere bio-accumulates in the environment and can cause impaired neurological development in fetuses, infants and children, as well as problems in the nervous system and gastrointestinal tract in adults (7), to name but a few adverse health effects. In 2000, the EPA announced its intent to regulate HAP emissions from coal- and oil-fired power plants. In March of 2005, EPA issued the Clean Air Mercury Rule (CAMR) to permanently cap and reduce mercury emissions from coal-fired power plants. This rule made the US the first country in the world to regulate mercury emissions from utilities. While a federal court invalidated the CAMR in February of 2008, there is no doubt of the urgency to reduce our mercury emissions to the environment. Based on research conducted by the EPA, coal-fired power plants emit 50 tons of mercury annually (8). It is important to develop cost-effective

technologies that efficiently remove mercury from the flue gas of power plants to avoid significant harm to the long-term health of the nation. The EPA has announced its intent to impose mercury emissions rules requiring power plants to reduce their mercury emissions by 91 percent (9). The annual cost to meet the new regulation will be approximately $11 billion in 2016. However, the public-health benefits are estimated to be between $59 billion and $140 billion in 2016, much of it from avoiding premature deaths (10).

Mercury is truly a global pollutant, as Hg^0 has an atmospheric lifetime of ca. 1-2 years and can travel over great distances (11, 12). Mercury emitted from a coal combustion power plant in China can thus be deposited in the United States and vice versa. In this global context, mercury removal from coal combustion flue gas is especially important considering the total mercury emission from coal combustion in China: 302.87 tons in 1995 (13).

The flue gas in coal combustion contains gases such as SO_2, NO_x, and chlorine as well as toxic metals such as arsenic, lead, selenium, thallium, and mercury, all of which have adverse effects on human health (14). While pollutant control devices such as flue gas desulfurization (FGD) scrubbers are used to remove SO_2, and selective catalytic reactors (SCR) are used to remove NO_x, heavy metals removal techniques from coal combustion power plants have yet to be implemented in a widespread manner in the United States.

The current best available technology for mercury capture is activated carbon injection; however, it does have several limitations, such as weakened performance when exposed to sulfur species (SO_x) in the flue gas and high operating cost (15-18).

This work focused on the optimization of mercury removal under simulated flue gas conditions whereby flue gas components (NO_2, SO_2, and HCl), temperature, moisture, and contact time were chosen as the main parameters.

Specifically, this research focused on the use of a photocatalytic material, silica-titania composite coated onto ceramic chemical tower packing material (STCP). Previous research involving UV irradiation of silica-titania composite (STC) in pellet form was conducted and was successfully shown to remove mercury from air (19, 20). The STCP material, which has a higher void space than STC pellets, was conceived as a way to improve the scalability of this technology for application in a power plant by reducing pressure drop through the reactor (i.e. tower packing has more void space than a fixed bed of pellets), minimizing the energy necessary to push the air stream through the system and thus decreasing operating and maintenance cost.

A reactor containing the STCP material to oxidize and remove mercury could be inserted into the air stream of a power plant after the particulate control devices (fabric filter or electro-static precipitator) and before the stack. In this fashion, the build-up of fly ash and other particulates would be mitigated. The treated air stream would then exit the power plant through the stack.

With the goal of evaluating the STCP material for full-scale application in mercury removal from coal combustion flue gas, the following hypotheses and objectives were identified.

The following hypotheses were investigated in this study:

- Mercury oxidation could occur under UV irradiation alone at wavelengths lower than 365 nm, as wavelengths above that lack sufficient energy to oxidize mercury.

- STC in pellet form has been shown to oxidize and remove mercury successfully from air. Therefore, it is expected that the STCP is capable of oxidizing and removing mercury from simulated coal combustion flue gas at similar levels.

- The STCP material would not be affected by catalyst poisoning from sulfur and NO_2.

The objectives of this work were as follows:

- Study of oxidation of Hg by UV alone. This has not been previously studied. Wavelengths of 365, 254, and 185 nm were examined for their ability to oxidize Hg while varying contact times in the reactor and moisture content in the air stream.

- Test performance of STCP under simulated flue gas conditions.

- Conduct long-term experiments (> 200 hours) to evaluate the prolonged exposure of STCP to sulfur and NO_2.

- Characterize STCP surface using various techniques (SEM, nitrogen adsorption isotherm, XRD).

- Perform durability tests on STCP.

CHAPTER 2
LITERATURE REVIEW

Photocatalysis

Upon absorption of a photon with an energy (*hv*) greater than or equal to the semiconductor's band gap energy, an electron/hole pair in the semiconductor is formed where an electron (e^-) is promoted to the conduction band and leaves behind a hole (h^+) in the valence band (Equation 2-1, Figure 2-1) (21, 22):

$$TiO_2 + hv \rightarrow TiO_2 (e_{CB}^- + h_{VB}^+) \quad (2\text{-}1)$$

These electron/hole pairs are able to generate heat when recombined or subsequently contribute in redox reactions. Excited electrons participate in reduction reactions of compounds adsorbed to the semiconductor surface; however, they can also react with oxygen and via intermediate reactions create H_2O_2 and OH* radicals that are known to be powerful oxidizers. The formation of these compounds can be seen in Equations 2-2 through 2-7 (23):

$$TiO_2(e_{CB}^-) + O_2 \rightarrow TiO_2 + O_2^- \quad (2\text{-}2)$$

$$O_2^- + H^+ \rightarrow HO_2 \quad (2\text{-}3)$$

$$HO_2 + HO_2 \rightarrow H_2O_2 + O_2 \quad (2\text{-}4)$$

$$TiO_2(e_{CB}^-) + H_2O_2 \rightarrow TiO_2 + OH^* + OH^- \quad (2\text{-}5)$$

$$H_2O_2 + O_2^- \rightarrow OH^* + OH^- + O_2 \quad (2\text{-}6)$$

$$H_2O_2 + hv \rightarrow 2OH^* \quad (2\text{-}7)$$

It is also believed that the hole in the valence band contributes to oxidation of contaminants through the formation of OH* radicals. This can be seen in Equations 2-8 and 2-9 (23):

$$TiO_2(h_{VB}^+) + H_2O \rightarrow TiO_2 + OH^* + H^+ \quad (2\text{-}8)$$

$TiO_2(h_{VB}^+) + OH^- \rightarrow TiO_2 + OH^*$ (2-9)

OH* radicals can then oxidize organics as well as inorganics such as mercury to a final form of mercury oxide (24, 25).

Methods of Mercury Removal

Mercury is a d-block element, in the groups 3 through 12 of periodic table known as transitional elements. It has an electronic structure that causes it to be unusually nonreactive compared to other metals ($5d^{10}6s^2$ closed shell that is isoelectric to He), and especially difficult to oxidize without the presence of strong oxidants such as Cl_2 (26, 27). Mercury has three oxidation states, elemental (Hg^0), and two ionic states (Hg^+ and Hg^{2+}), and can also occur as particulate mercury (Hg^p). Particularly in its elemental form, mercury remains in the atmosphere for an extended period of time, contributing to the global background concentration, while in its oxidized forms it can be associated with particles or occur as gases, and are more readily deposited (28). The oxidation state of mercury is difficult to predict; its state is highly dependent on the type of coal burned, as well as the configuration of air pollution control devices (APCD) in a given plant (29-33). For example, coals low in chlorine lead to a greater proportion of elemental mercury (vs. oxidized). This form of mercury cannot be effectively captured in particulate control devices such as electrostatic precipitators (ESP) because it is present as a vapor in combustion systems. Nor can it be removed by flue gas desulfurization scrubbers (FGD) because it is not very soluble in water (34).

Much work has been done to develop models that can predict mercury speciation in flue gas streams of various power plant configurations (33, 35-40), and thus devise a removal technology that can be used throughout the electric utility industry (41). Fundamentally, two types of removal technologies exist: those based on adsorption

alone and those that aim to convert all mercury in the air stream into the much more reactive and removable mercuric species by means of oxidation, with adsorption either simultaneously occurring or in a subsequent stage.

The current maximum achievable control technology (MACT) is activated carbon injection (ACI). Powdered activated carbon is injected upstream of a particulate matter (PM) control device, such as a fabric filter, and adsorbs mercury. The contaminated carbon is then captured in the fabric filter and removed from the plant. Because it commingles with fly ash in the fabric filter and cannot be easily separated, the salability of the fly ash is adversely impacted, increasing the operating cost of ACI beyond just that of the material. Other sorbents such as calcium have been investigated, but have been found to be ineffective in removing elemental mercury (42).

Gold and palladium catalysts have also been tested on bench-scale, but in their current technical development are not suitable for combustion conditions for several reasons. Gold catalysts do not adsorb mercury efficiently at temperatures higher than ca. 390°F (43), and were found to desorb mercury above 930°F (44), which can easily be achieved during a temperature excursion. Fouling is a definite issue with flue gas, which contains multiple corrosive constituents such as NO_2, SO_2, SO_3, Cl_2, and HCl. While less of a problem with gold, catalyst deactivation seemed more pronounced with palladium catalysts (45, 46). While activated carbon can overcome the fouling issue by virtue of its short contact time with the flue gas, sorbents and catalysts that remain in contact with the gas stream for any significant period of time are exposed to the aforementioned corrosive constituents and fly ash that deposit on any and every surface

(47). Similar problems were found to exist with selective catalytic reduction (SCR), normally used for NO_x removal, when applied to mercury oxidation (48).

While multi-pollutant controls, i.e. the combination of SCR, wet FGD and PM controls, are being implemented more and more in the US and are already common in certain countries in Europe, and have an inherent mercury removal of 70% or more (31, 37), this is not an optimal approach for two reasons. First, the greater removal values were achieved by plants burning higher rank coals such as bituminous, which have a higher chlorine concentration and lower sulfur concentration than lower rank coals. Thus, the formation of mercuric oxide species by chlorine species is promoted post-combustion (40), which can be captured in wet FGDs. Consequently, plants burning lower rank coals (sub-bituminous, lignite, or blends), will see lower removal rates because of a matrix with little chlorine and/or high sulfur content (49), resulting in elemental mercury dominant in the air stream and little removal. Second, it is expected that future regulations will stipulate a mercury removal efficiency of at least 90% (10). In that scenario, ACI can easily become a major financial burden for electric utilities and consumers alike.

Silica-Titania Composites

The STC technology was developed to treat VOCs. In addition, it has also been found to be effective for mercury removal in a bench-scale reactor and in chlor-alkali facilities (19, 25, 50-52).

A STC system was developed that would oxidize and adsorb mercury in one stage in a packed bed. A thorough description of STC synthesis can be found elsewhere (53, 54). STC in the form of pellets was primarily used, with titanium dioxide (TiO_2) used as the photooxidization component. Silica was chosen as the substrate because of its high

surface area (53). While elemental mercury (Hg^0) adsorbs onto the pellet surface, UV irradiation activates the titania; electron-hole pairs are generated that can oxidize the adsorbed mercury. A lower volatile form is created, HgO, which is not as easily re-entrained as Hg^0. For these reasons, the composite was found to develop an enhanced adsorption capacity after periods of photocatalytic oxidation (25).

Previous research investigated performance of STC under various conditions, such as relative humidity of the carrier gas, TiO_2 loading, and fixed bed residence time (19, 20, 25, 55). A UV lamp with a nominal wavelength of 350 nm was cycled off and on (19). With UV initially off, mercury was loaded onto the pellets until the effluent reached 68% of the concentration of the influent, at which point the UV lamps were turned on. Hg removal of greater than 95% was observed during the UV-on phase at low relative humidity (15%), while high moisture (greater than 75% RH) reduced adsorption capacity by occupying active sites on the adsorbent. A 13% TiO_2 loading was found to be optimal based on current synthesis technology. These results were obtained at a temperature of 80°F and with breathing grade air, mercury, and nitrogen as the balance gas making up the air stream. In a combustion system such as a coal-fired power plant, temperatures are much higher (> 250°F) and the air stream contains a multitude of gases (and particulate matter which was not investigated).

At 250°F under dry conditions (i.e. no addition of moisture), removal efficiency during UV irradiation was greater than 95% for the clean gas, and was not affected when NO_2, HCl, or SO_2 were added (19). When water vapor was added (1.8% relative humidity) and with a temperature of 250°F, UV irradiation significantly improved removal

efficiency as compared to no UV. When constituent gases were added, there was little change in Hg removal performance under UV-irradiated conditions.

The effect of water vapor was subsequently investigated with respect to adsorption, oxidation and reemission of the adsorbed mercury back into the air stream (55). At 150°F, moisture was found to inhibit both adsorption and photocatalytic oxidation, as well as promote reemission of adsorbed Hg^0. It was found that continuous UV irradiation in humid air could either inhibit or promote Hg^0 reemission, depending on the dominant reactions occurring on the STC surface: when photocatalytic oxidation of reemitted Hg^0 was dominant, UV was an inhibitor, but as the hydrophilic surface attracted water vapor, which blocked the photo-oxidizing reagent TiO_2, UV acted as a promoter for Hg^0 reemission as the reduction of HgO to Hg^0 dominated (55). It is clear that water vapor plays a key role in the removal of Hg from the air stream by affecting the dynamic equilibrium that exists between Hg adsorption and reemission.

The STC material has been characterized in terms of its photocatalytic oxidation kinetics, and good agreement with the Langmuir-Hinshelwood (L-H) model was demonstrated (56). The rate of Hg^0 oxidation increased as the influent concentration increased, and was greatest without addition of moisture. This would appear to agree with previous research (19).

Mercury Oxidation

The reaction occurring between mercury and oxygen in the presence of 253.7-nm light is given by Equation 2-10:

$$Hg + 2O_2 + 253.7 \text{ nm light} \longrightarrow HgO + O_3 \quad (2\text{-}10)$$

The reaction products are mercuric oxide as well as ozone, because Hg^0 serves as a sensitizer for ozone formation and ozone oxidizes mercury (57). This has been shown to be a potential method of mercury removal from coal combustion flue gases (58, 59), and warrants further investigation.

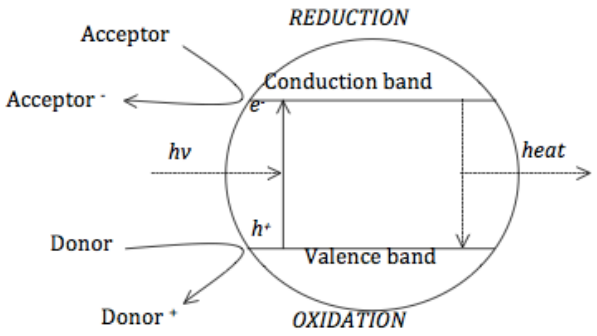

Figure 2-1. Schematic of band gap irradiation of a semiconductor particle

CHAPTER 3
EXPERIMENTAL

STCP Production

STC was coated onto packing material (LPD® KNIGHT-CHEM® Chemical Porcelain Packing) by preparing a silica suspension (50% Ludox colloidal silica, 50% DI water mixed with 3.5% TiO_2 by weight), in which the packing material was dipped and then dried in an oven. The TiO_2 used was commercially available Degussa P25. This coating procedure was repeated up to 22 times to produce a visually uniform coating, and was tested for hardness and durability. Polyethylene glycol (PEG) was added as a binding agent and compared to the former suspension, but no significant performance differences were observed. In addition, the coating was not noticeably thicker or more uniform with the solution containing PEG.

Characterization

The STCP material was characterized using scanning electron microscopy (SEM). SEM functions by sending a stream of electrons (confined and focused by apertures and magnetic lenses into a monochromatic beam) towards a sample using a positive electrical potential. The resulting interactions between the electrons and the sample are detected and transformed into an image. A high vacuum SEM needs a very low pressure in the sample chamber (below 10^{-4} Pa) in order to function. This reduces the number of collisions between the beam electrons and the molecules of the residual gas, thus minimizing noise in the image. The sample must either be inherently conductive or otherwise be coated with a conductive material to minimize charging of the sample, conduct away heat from the sample during imaging, and increase the secondary electron yield of the sample.

Another characterization technique employed in this research was gas adsorption isotherms, using a Quantachrome® NOVA 2200e (Boynton Beach, FL). Using the Brunauer, Emmett, and Teller (BET) method and classical Kelvin equation, the surface area, total pore volume, and pore size can be determined. A sample is exposed to nitrogen gas, which is added or removed from the sample chamber in finite volumes at carefully controlled pressures. The result is a data plot of the quantity of adsorbed gas versus the equilibrium pressure, the isotherm plot. Based on the plot and amount of adsorbed gas, the values of the aforementioned properties can be calculated.

X-ray diffraction (XRD) is a technique used to identify crystalline materials by directing a focused X-ray beam onto a sample. Bragg's Law ($n\lambda=2d\sin\theta$) can be applied to determine the distances (d) between the planes of the atoms that make up the sample, as the wavelength (λ) of the incident X-ray beam is known and the angle of incidence (θ) can be measured (n is the order of the diffracted beam). As the STCP is a mixture, XRD analysis can determine the proportion of different components. The degree of crystallinity can also be determined, which would make it useful in determining the proportion of anatase TiO_2 on the surface of the STCP.

Experimental Setup

The experimental setups used to collect the mercury oxidation and removal data can be seen in Figures (3-1) and (3-2). Air from a compressed air tank (Airgas) is run through Pyrex tubing wrapped in heat tape and the temperature was controlled with a power controller and measured with thermocouples placed throughout the test stand. Both gas flow rate and the flow rate of water into the system are controlled by rotameters (Aarlborg, various models). Flow rates were determined based on the desired contact time in the reactor and the target concentrations of the constituents.

Mercury was introduced into the system by passing nitrogen gas over an elemental mercury-containing bubbler in a heated water bath (maintained at 106°F) to prevent fluctuation in mercury delivery. The water vapor concentration is controlled by injecting de-ionized (DI) water (18.1 MΩ-cm) from a pressure vessel into the heated main line, where it immediately vaporizes.

The 100 mL Pyrex annular reactor with a quartz sleeve for UV irradiation is sufficiently spaced from the main line to allow mixing of the gas constituents to occur. The inside of the reactor is approximately 14 cm long and the quartz sleeve is 2.5 cm in diameter. There is a space of approximately 0.8 cm between the outside of the quartz sleeve and the inside of the reactor. The reactor, tubing leading to it, and the tubing following it, are all wrapped in heat tape to maintain constant temperatures in the test stand. Teflon tubing was used on all lines that were not Pyrex to avoid adsorption of mercury.

Experiments were conducted at least twice to determine standard error, which is depicted by error bars in figures demonstrating mercury oxidation or removal experiments.

Oxidation Studies

Mercury oxidation by UV alone was examined initially to determine the benefit when compared with photocatalytic oxidation. Wavelengths of 365 nm, 254 nm, and 185 nm were chosen, the latter two were lower than the 365 nm wavelength examined in previous literature (56, 60). All lamps were germicidal and manufactured by Atlantic Ultraviolet Corporation.

The ozone output of the 185 nm bulb was measured at the temperatures examined in this study using an ozone monitor (Teledyne Model 454). Using an ozone

generator (Pacific Ozone Technology), that ozone dosage could then be applied to a mercury-laden air stream in the absence of UV. Experiments could thus be conducted at the same contact times and moisture conditions as with the UV lamps.

Flue Gas Simulation

To simulate flue gas, individual flue gas components are added to the main line, prior to the heated section. The main air stream temperature was chosen similar to post-ESP flue gas conditions, and experiments conducted at both 275° and 375°F. Flue gas components selected include NO_2, SO_2, and HCl, and were selected based on their importance in the mercury oxidation/removal chemistry and occurrence in coal combustion scenarios (31). While NO is the predominant form of NO_x in actual flue gas, NO_2 was chosen in this study, and was expected to decompose into a mixture of NO and NO_2 when introduced into the heated main line, as NO_2 decomposes above 300°F (26). Concentrations of the flue gas components were chosen based on conversations with a lignite coal-firing utility operator and their observed concentrations: 250 ppm_v NO_2, 350 ppm_v SO_2, and 100 ppm_v HCl. SO_2 and NO_2 were introduced via gas tanks. Chlorine was introduced by mixing liquid HCl with water in the pressure vessel. Due to the nature of HCl, there are several chlorine species in the gas mixture, such as HCl, HOCl and Cl_2 (61-63). The mercury concentration was kept at around 10 ppb (90 $\mu g\ m^{-3}$), which is similar to the concentrations observed under actual flue gas conditions (41). To account for the fluctuation of the influent concentration (10-15% around the target concentration), regular influent samples were taken during runs.

A wavelength of 254 nm was used for STCP experiments after it was determined by experimentation that 185 nm did not offer significantly improved performance, while increasing energy costs, making it less economical in industrial application. Relative

humidity was kept constant between temperatures at 4% RH as this is still within the range seen at coal combustion power plants. This translates into water vapor concentrations (WVC) of 43,000 ppm_v for experiments conducted at 275°F and 197,000 ppm_v for the 375°F experiments.

Mercury Analysis

A junction after the reactor (Figures 3-1 and 3-2) allowed for the effluent air to be directed to the appropriate point of analysis, either an influent or an effluent measurement. The excess air was exhausted to a carbon trap. The instrument used to measure mercury was an Ohio Lumex® Zeeman Mercury Analyzer (RA-915+), hereafter called Zeeman, which measures gaseous elemental mercury in real-time using the principle of atomic absorption spectrometry to detect and quantify mercury. The method of mercury analysis was the use of a Zeeman with chilled impingers in front of it to determine mercury speciation and remove the corrosive gases from the air stream, such as chlorine, NO_2, and SO_2 (Figure 3-3). Once the air stream was treated in the reactor it reaches a junction, where it can either be sent through an impinger train design to determine elemental mercury or an impinger train to determine total mercury concentration. Both impinger trains contained a NaOH impinger to remove corrosive gases (64). The elemental mercury train then followed the NaOH impinger with an impinger containing a KCl solution in order to remove oxidized mercury and thus only allowed elemental mercury through the Zeeman. The impinger train designed to measure total mercury had an impinger containing a $SnCl_2$ solution, which reduced all oxidized mercury to elemental mercury, allowing the Zeeman to measure the total concentration of the mercury in the air stream. Prior to entering the Zeeman, both

impinger trains pass the air stream through a condensation impinger to avoid condensation in the Zeeman.

Mercury removal was calculated using total mercury concentrations and equation (3-1). Mercury oxidation was calculated using equation (3-2), whereby the total mercury concentration of the influent and the elemental mercury concentration of the effluent are measured.

$$\text{Hg Removal} = \frac{[Hg_{total}]_{Influent} - [Hg_{total}]_{Effluent}}{[Hg_{total}]_{Influent}} \times 100 \quad (3\text{-}1)$$

$$\text{Hg Oxidation} = \frac{[Hg_{total}]_{Influent} - [Hg^{0}]_{Effluent}}{[Hg_{total}]_{Influent}} \times 100 \quad (3\text{-}2)$$

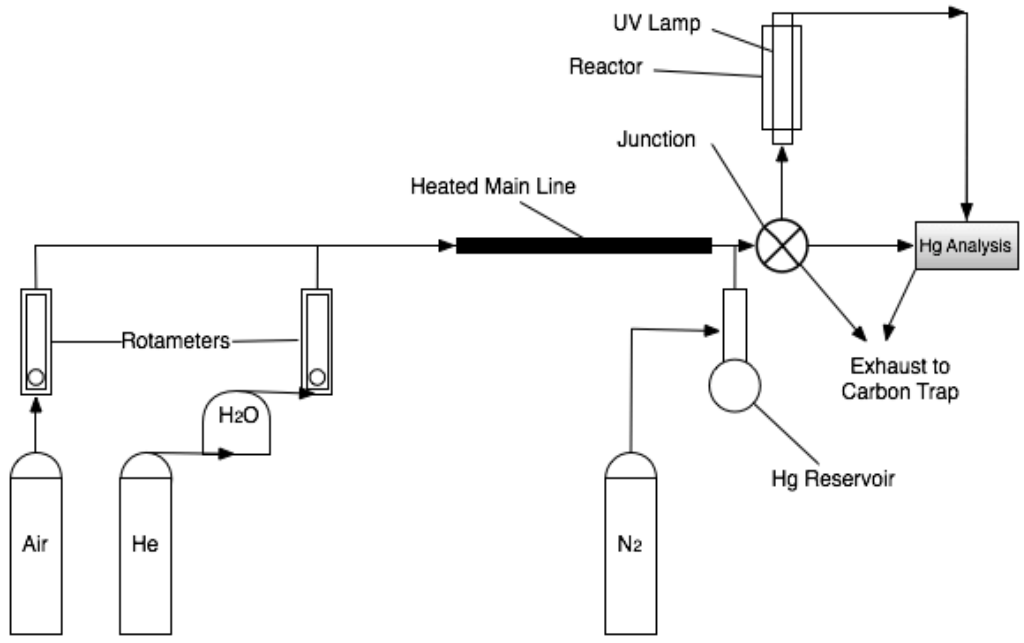

Figure 3-1. Test stand setup for mercury oxidation study

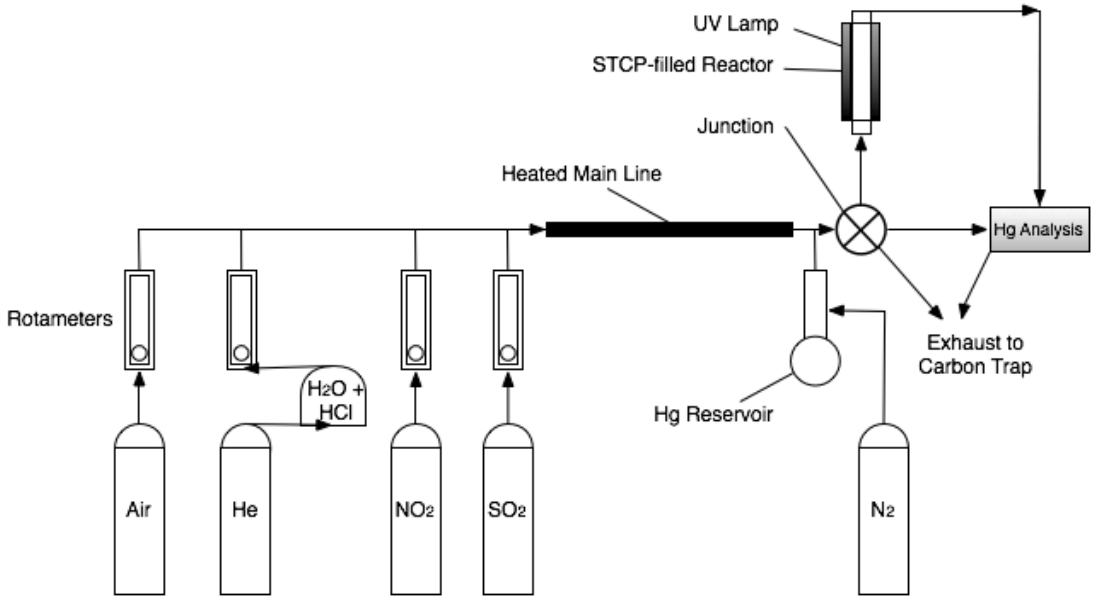

Figure 3-2. Test stand setup for STCP study

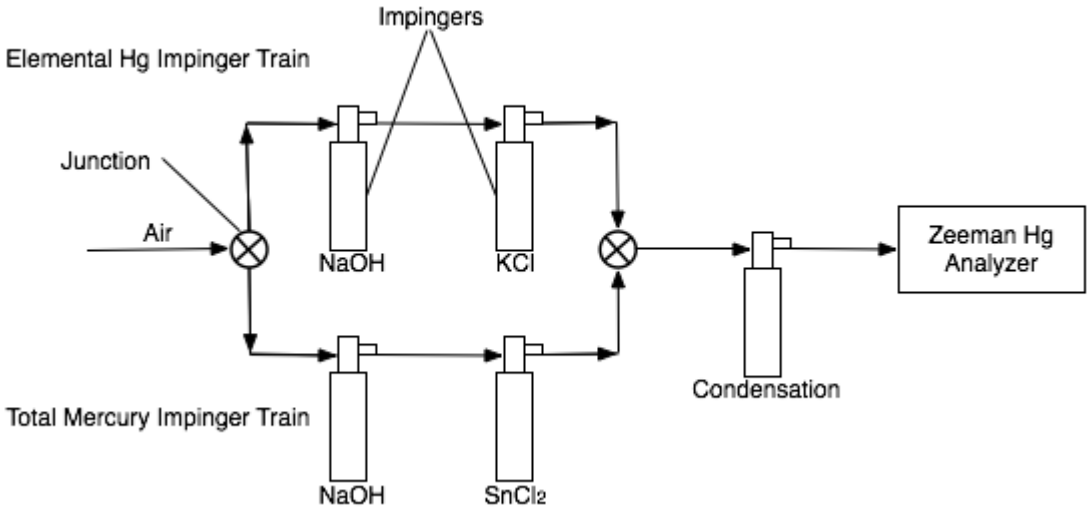

Figure 3-3. Hg analysis setup with impingers and Zeeman

CHAPTER 4
MERCURY OXIDATION BY UV

Several approaches exist to oxidize Hg^0, either by non-thermal plasma (65), achieving mercury oxidation of 59%; corona discharge (66), whereby an air stream is passed through a field of ionized gas and mercury oxidation of 86% is achievable; ozone (67), or UV irradiation (58, 59). UV irradiation as a means to oxidize mercury was studied at 254 nm with simulated flue gas, at temperatures between 80°F and 350°F (58), and focused on the effects of gas components (SO_2, NO), as well as light intensity. The study found that mercury was most easily removed at temperatures below 300°F and that NO negatively affected removal. A separate study of mercury oxidation at 100°F and 280°F also used 254 nm UV light and simulated flue gas (59). This study also found that a temperature increase and the presence of NO had negative effects on mercury oxidation. In both studies, UV wavelength and water vapor concentration were not varied.

Herein, the objective was to investigate UV wavelength, contact time, temperature, and water vapor concentration on mercury oxidation to understand the viability of this approach for application in mercury removal in a pre-FGD treatment system.

Effect of Contact Time

Contact time is an important design factor in designing flue gas purification systems, as a shorter contact time allows for a smaller reactor volume, keeping costs down. In this study, it was necessary to determine the minimum contact time required to achieve at least 91% mercury oxidation, as this is the mercury removal required by the United States Environmental Protection Agency (EPA) in announced future regulation (10). Contact times in the annular reactor in this study were varied from 0.3

to 1.5 seconds, similar to those found in treatment systems of coal combustion power plants.

Oxidation was expected to increase as the contact time increased, which was confirmed (Figures 4-1 and 4-2). Figure 4-1 shows mercury oxidation by the 254 nm UV bulb at 300°F and a water vapor concentration (WVC) of 26,000 ppm_v. Oxidation reached 86% at a 1.2 second contact time. At a UV wavelength of 185 nm and the same WVC and temperature (Figure 4-2), there was a greater level of mercury oxidation at contact times under one second than at the same contact times with 254 nm UV. However, mercury oxidation did not exceed 91% until a contact time of 1.2 seconds. The Reynolds numbers vary from 440 down to 90 for the 0.3 and 1.5 second contact times, respectively, indicating laminar flow. This might explain the low oxidation at the shorter contact times, as there may be a channeling effect causing a lower level of mixing in the annular reactor.

Effect of Water Vapor and Temperature

Flue gas conditions are subject to change, as the coal being burnt is a heterogeneous material, which can result in fluctuations in the concentration of water vapor in the air stream. Therefore, it was important to determine the change in mercury oxidation by the UV bulbs as WVC was varied.

When irradiated with 365 nm UV, oxidation was minimal over a range of temperatures and WVCs (Figures 4-3, 4-4, and 4-5), likely because it lacks sufficient energy to excite mercury electrons to the conduction band (68). Figure 4-3 shows Hg oxidation at 80°F over three UV wavelengths and several WVCs at a contact time of 1.2 s. At that temperature there is a clear difference between the performances of the 254 nm versus the 185 nm lamps, whereby the 185 nm lamp maintains a greater level

of Hg oxidation over the range of WVCs. As the 185 nm lamp is ozone-producing, it is possible that the ozone aids in Hg oxidation. There is a significant decline in oxidation for 185 nm UV with an increase in WVC, possibly due to the overabundance of water vapor, interacting with UV light. However, the decline is steeper than for 254 nm. The increased sensitivity of the 185 nm bulb to water vapor is possibly due to water vapor impeding ozone formation by the bulb (69). At a UV wavelength 254 nm, Hg oxidation shows an improvement as the water vapor concentration increased until about 14,000 ppm_v (40% relative humidity), at which point oxidation drops slightly. Here, water vapor aided in oxidation through formation of OH* radicals by UV irradiation (70) while not inhibiting the interaction of the radicals with Hg^0. These OH* radicals are formed through the photolysis of water by UV irradiation. The radicals subsequently aid in the oxidation of mercury (71). As WVC further increased, the water vapor-UV interaction negatively affects oxidation (Figures 4-3 and 4-5). In Figure 4-4, that point does not seem to have been reached, as mercury oxidation still increased at the highest WVC studied.

Figures 4-4 and 4-5 show Hg oxidation at 1.2 s contact times and temperatures of 200°F and 300°F, respectively. At both temperatures, UV 254 showed less oxidation at the very lowest WVC, but was clearly aided by the presence of water vapor as WVC increased, likely due to the formation of OH* radicals as discussed above. In fact, when comparing the oxidation at 26,000 ppm_v WVC and 1.2 s contact time in Figure 4-1 with the oxidation at 3 ppm_v WVC at the same contact time in Figure 4-5 (data point with the lowest WVC), mercury oxidation jumps from just below 40% at 3 ppm_v to ca. 85% at 26,000 ppm_v.

Effect of UV

This study varied UV wavelength to determine the advantage, in terms of mercury oxidation, a 185 nm bulb might have over a 254 nm bulb. At 200°F and 300°F, UV wavelength has a clear effect on mercury oxidation rates only in the lower range of water vapor concentrations. In both Figure 4-4 and 4-5, Hg oxidation did not significantly change over the range of WVCs when utilizing the 185 nm UV lamp. While oxidation started out much higher than that of the 254 nm lamp at the low range of WVC, both lamps perform similarly at higher WVCs. This is contrary to what would initially be expected, as ozone should provide for additional oxidation. However as previously discussed, water vapor can impede ozone formation by the185 nm bulb (69), rendering an ozone-producing lamp no more useful than an “ordinary” UV lamp at high temperatures and water vapor concentrations.

At 300°F (Figure 4-5), 254 nm UV showed better oxidation compared to 200°F, likely due to the increased Brownian motion inside the reactor, which aids the interaction between OH* radicals and Hg^0. With both lamps, a slight decrease in oxidation can be observed as WVC increased, as a consequence of the UV-water vapor interaction.

Effect of Ozone

The 185 nm bulb produced very little ozone at 80°F (0.01-0.03% by weight), therefore very little mercury oxidation was expected. Indeed, at that temperature, no detectable mercury oxidation by ozone alone occurred (Figure 4-6). At 200°F, ozone generation by the 185 nm bulb was highest (0.40% by weight), and mercury oxidation by that dosage of ozone was almost complete (i.e., almost 100%, Figure 4-7). Ozone generation by the 185 nm bulb was lower at 300°F (0.06% by weight), and resulted in

90-95% mercury oxidation by the corresponding ozone dosage (Figure 4-8). At both 200° and 300°F, these oxidation levels are higher than with the 185 nm bulb (Figures 4-4 and 4-5), suggesting interference between UV light and ozone, a phenomenon discussed in literature (55, 72, 73), in addition to the previously discussed effect of water vapor on ozone formation.

Summary

Oxidation of mercury at three UV wavelengths (365 nm, 254 nm and 185 nm) was investigated over a range of water vapor concentrations. Oxidation was higher with the 185 nm over the range of temperatures and water vapor concentrations than 254 nm, except at the highest WVCs and 200° and 300°F. There was no mercury oxidation with the 365 nm bulb in any conditions. With little water vapor in the air stream, oxidation at the 254 nm wavelength was low, but could be increased by an increase in water vapor concentration. Mercury oxidation at 185 nm was steadier over the range of water vapor concentrations tested, with decreasing levels of oxidation at the upper range of water vapor concentrations for all temperatures. Mercury oxidation of at least 90% was only achievable under certain scenarios under irradiation with 185 nm UV, where the water vapor concentrations were high enough to aid in the formation of OH* radicals, but not so high as to impede ozone formation. This study demonstrated the variability of mercury oxidation under UV irradiation, as well as the efficacy of this method for removing mercury in conjunction with a capturing mechanism, such as a wet FGD scrubber.

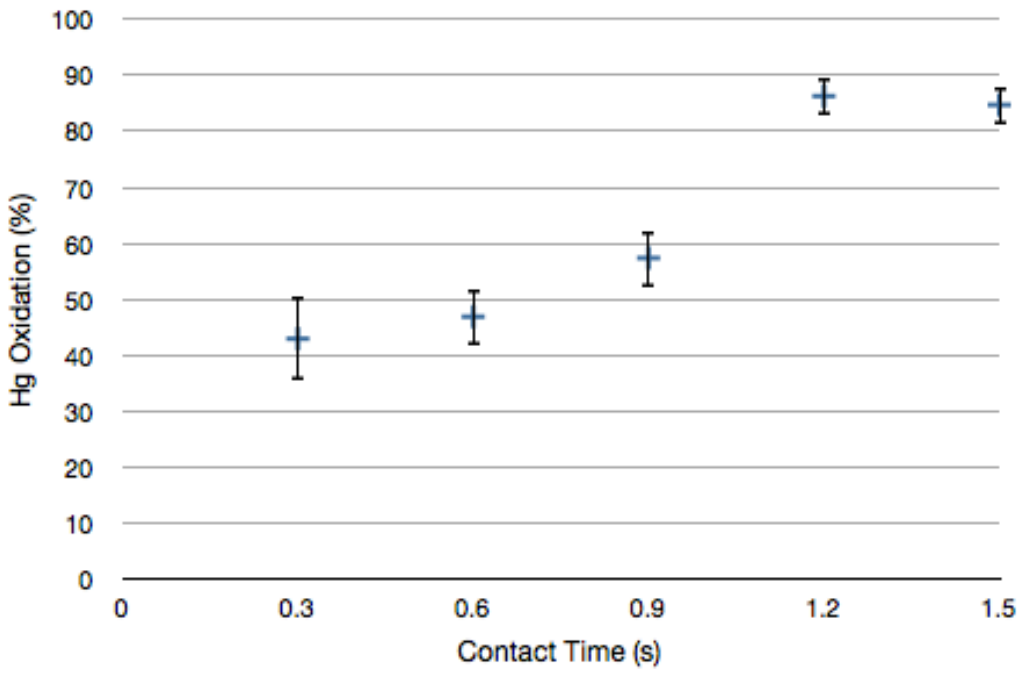

Figure 4-1. Mercury oxidation by 254 nm UV at 300°F and 26,000 ppm_v WVC.

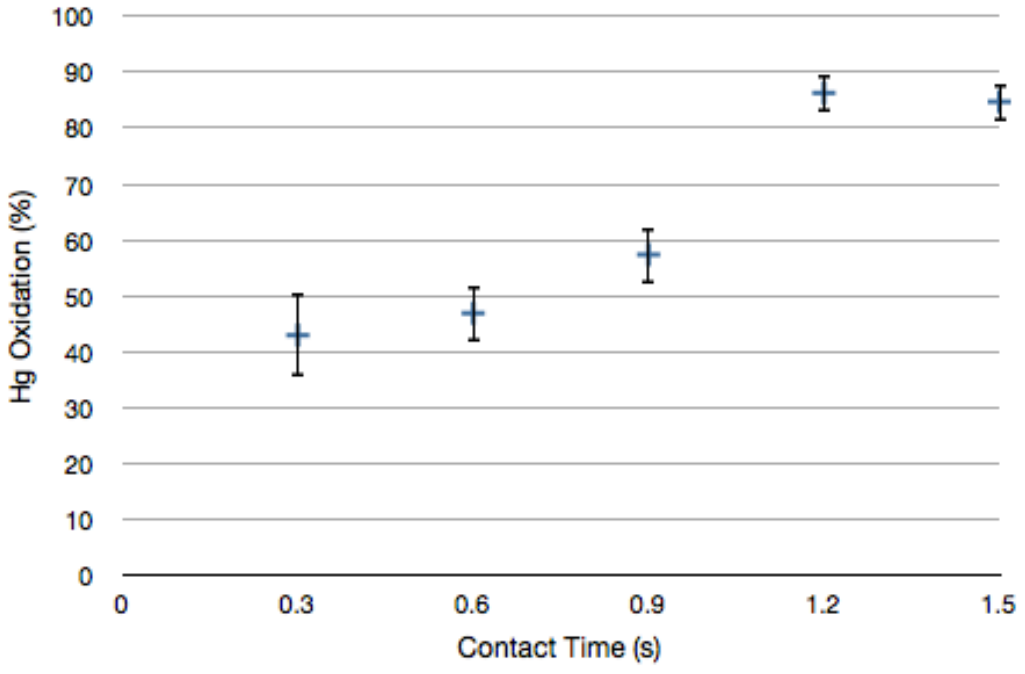

Figure 4-2. Mercury oxidation by 185 nm UV at 300°F and 26,000 ppm_v WVC.

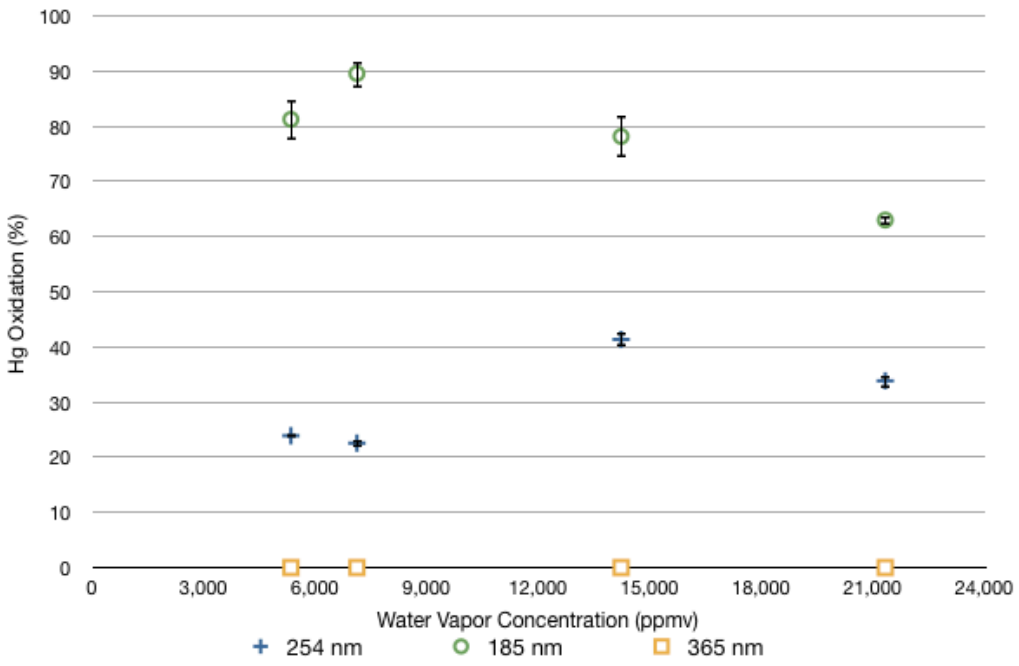

Figure 4-3. Mercury oxidation vs water vapor concentration varying UV wavelength at ca. 80°F.

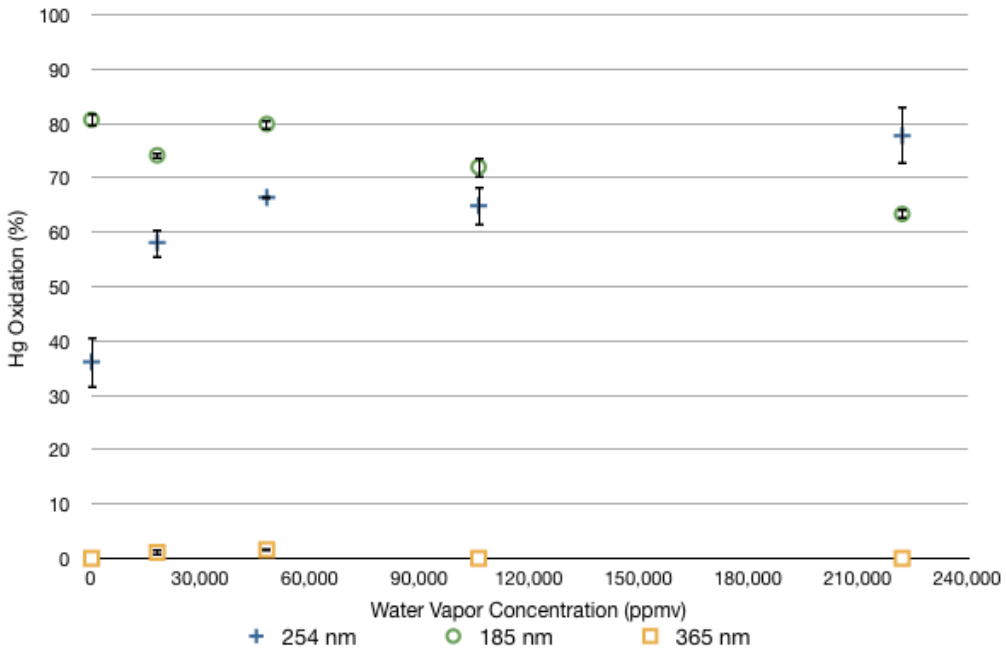

Figure 4-4. Mercury oxidation vs water concentration varying UV wavelength at 200º F.

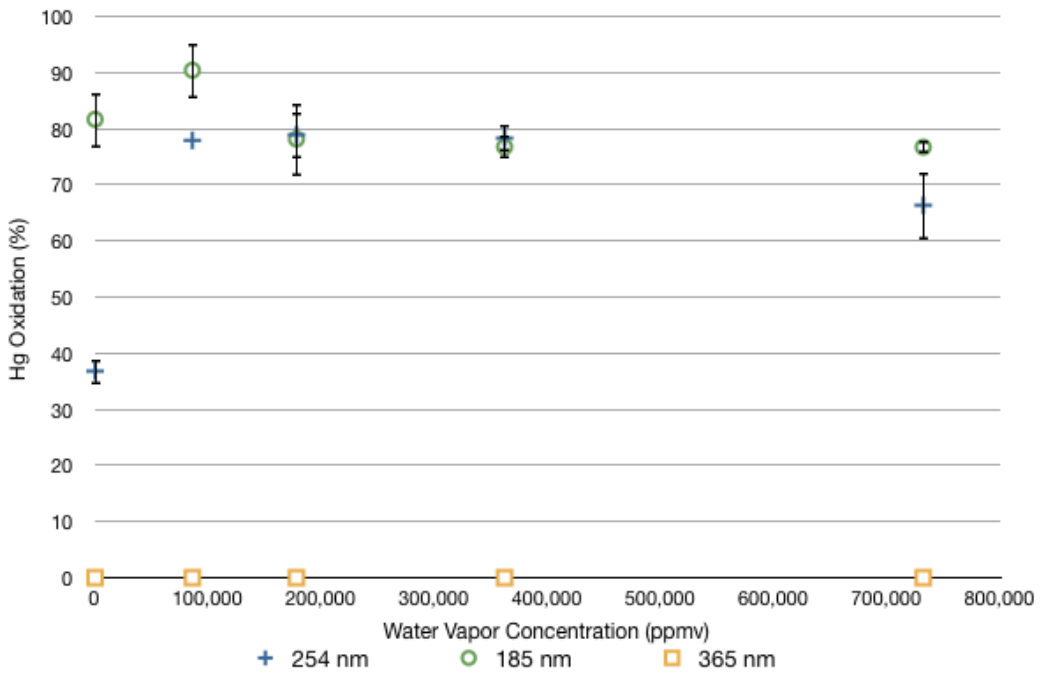

Figure 4-5. Mercury oxidation vs water concentration varying UV wavelength at 300°F.

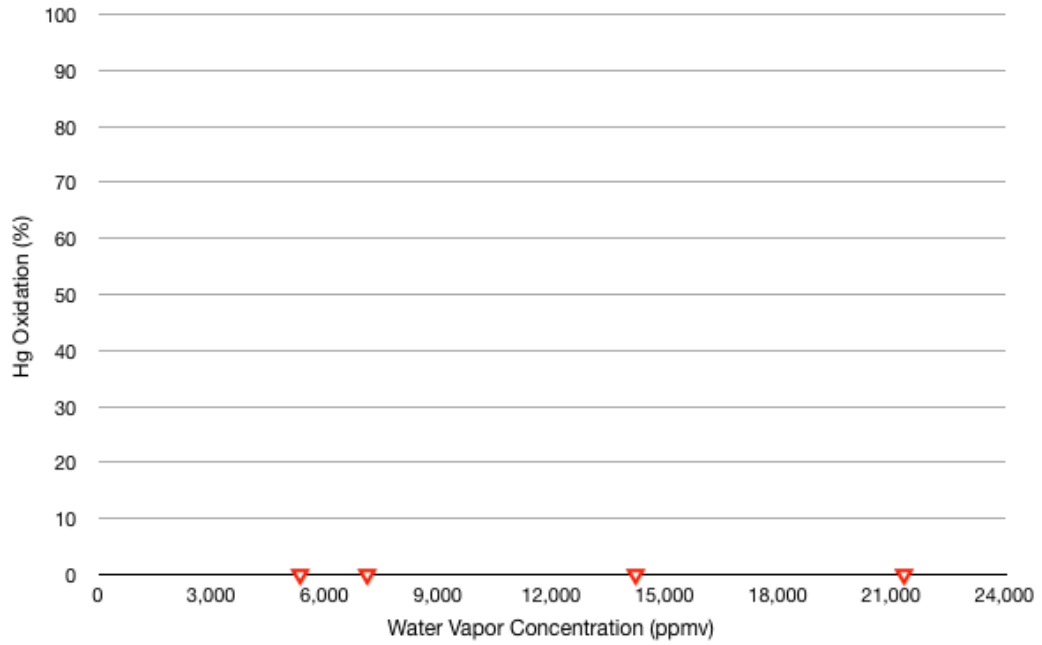

Figure 4-6. Mercury oxidation by ozone vs water concentration at ca. 80°F.

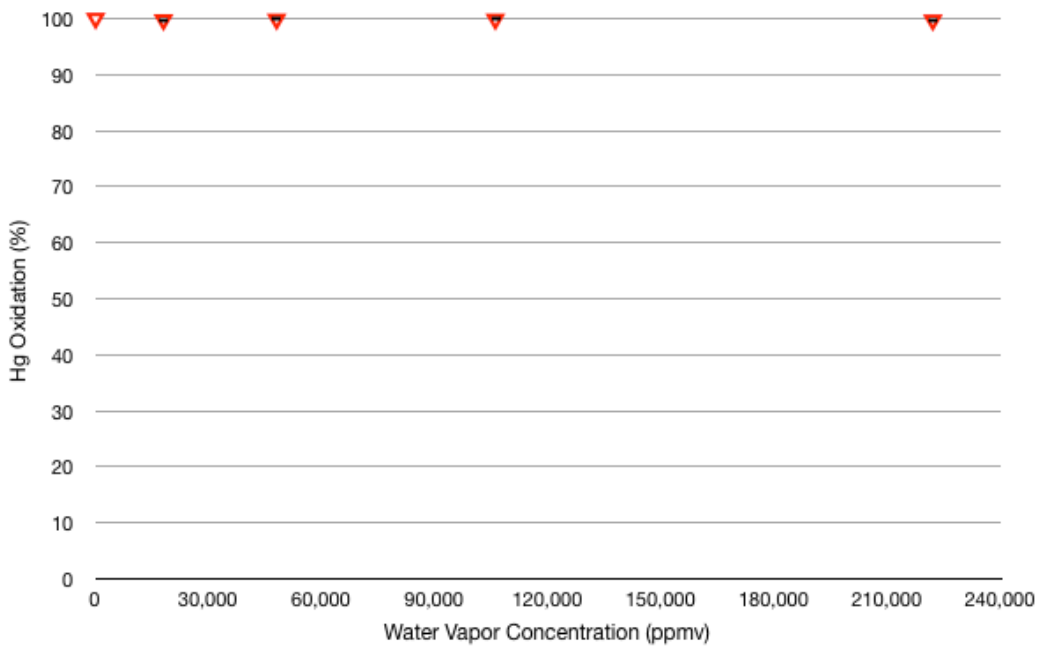

Figure 4-7. Mercury oxidation by ozone vs water concentration at 200°F.

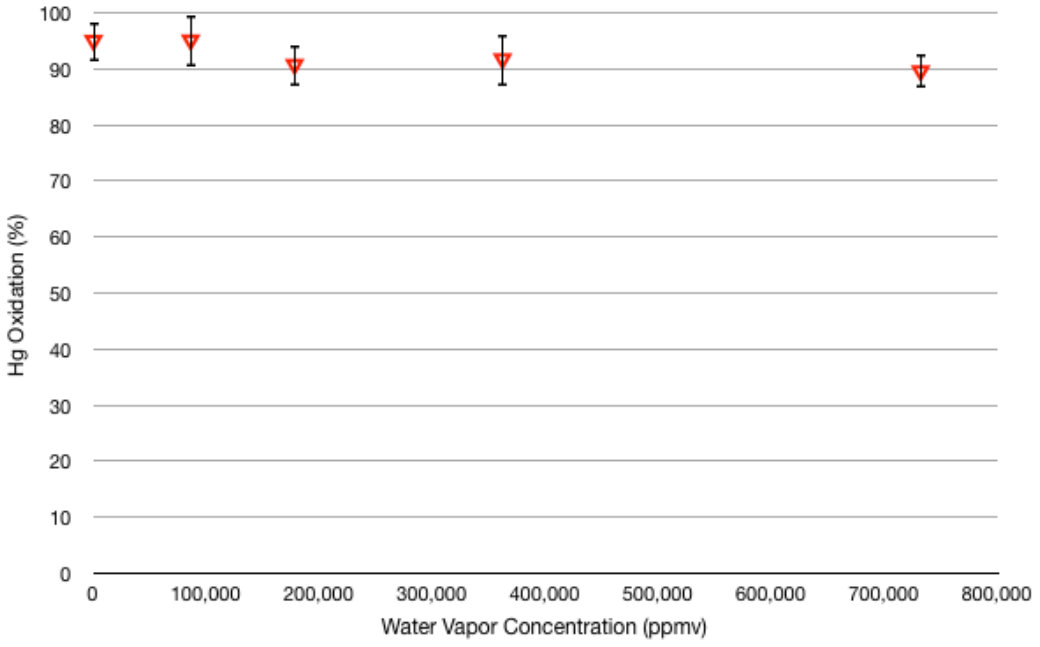

Figure 4-8. Mercury oxidation by ozone vs water concentration at 300°F.

CHAPTER 5
MERCURY VAPOR REMOVAL FROM BENCH-SCALE SIMULATED FLUE-GAS USING STCP

Currently, activated carbon injection is considered the most feasible technology by industry. However, a major drawback is the cost, as the injection rates to achieve high mercury removal performance can be very high and the mercury adsorption rate is dependent on flue gas conditions. A different strategy is multi-pollutant control, where technologies designed to remove other pollutants are utilized to additionally remove mercury and has been shown to be effective, in particular in systems with wet FGD scrubbers (41). This approach works well with high-rank coals, such as eastern bituminous, where there is a higher percentage of mercury in oxidized form present in the flue gas due to the higher chlorine content of the coal. Oxidized mercury is more water-soluble than elemental mercury (Hg^0) and thus more easily removed by a wet FGD scrubber. For low-rank coals, such as lignite or sub-bituminous, elemental mercury is the dominant species in the flue gas resulting in overall lower mercury removal efficiency from this approach.

A recent approach is the use of catalytic technologies to oxidize and remove mercury from coal combustion flue gas (32, 74, 75). The photocatalytic STC technology was developed to treat VOCs and in addition, it has also been found to be effective for mercury removal in a bench-scale reactor and in chlor-alkali facilities (19, 20, 25, 50-52, 55).

In this study, silica-titania coated packing (STCP) was developed, whereby the STC is coated onto ceramic chemical tower packing material. By reducing the surface area of hydrophilic silica in the STCP, it was thought this might reduce the effect of water vapor on the surface of the photocatalyst. Due to the materials higher void space

(i.e. the space not occupied by the material), this also allows for a lower pressure drop through the reactor than the STC in pellet form, and is thus economically more favorable. The goal of this study was to determine if the STCP is capable of oxidizing and removing mercury from simulated coal combustion flue gas with a performance similar to that of STC in pellet form. In order to test this, performance under simulated flue gas conditions was tested.

Baseline Experiments

Baseline experiments were conducted in order to determine the mercury removal without the presence of the flue gas constituents NO_2, SO_2, and HCl (Figure 5-1). Water vapor concentration was 43,000 ppm_v at 275°F and 197,000 ppm_v at 375°F (4% relative humidity). As can be seen in Figure 5-1, mercury removal remains at a steady state over a significant period of time. Lab work has shown steady state removal even after 200 hours of continuous runtime. Data points for both 275° and 375°F are shown (denoted as either “275” or “375” in the legend), with both no added water vapor (denoted as “0”) and added water vapor equaling 4% relative humidity (denoted as “4”). Addition of water vapor did not significantly affect mercury removal at 275°F. At 375°F however, there was a significant drop in mercury removal when water vapor was added. This is likely due to the significant increase in water content, which competes with mercury for adsorption onto the hydrophilic silica on the STCP surface.

Effect of NO_2

NO_2 was added to the air stream to determine its effect on mercury oxidation and removal. Figure 5-2 shows data with 250 ppm_v NO_2 (all other conditions equal to the baseline). Compared to the baseline (80% removal), there is a slight reduction in mercury removal to ca. 78%. NO_2 has been shown to enhance Hg oxidation on fly ash

(76), however to a minor extent as compared to chlorine addition. Therefore, the slight decrease in removal might be due to conversion of NO_2 to NO through UV irradiation, as NO has been shown to be an inhibitor of mercury removal by scavenging OH* radicals (20). Additional data confirmed that even after considerable run time (> 200 hours), removal stayed at ca. 78% (Figure 5-3).

Effect of SO_2

No significant change in removal occurred when SO_2 was added to the clean air stream, as can be seen in Figure 5-4. Whereas SO_X species (SO_2 and SO_3) are adsorption inhibitors in activated carbon injection (38), STCP performance showed little change when exposed to SO_2. This is possibly due to oxidization of SO_2 into sulfuric acid by UV irradiation in the presence of oxygen and water vapor (77). Even SO_2 that is adsorbed onto the STCP surface would not significantly affect mercury adsorption due to the higher adsorption capacity of the STCP material (300 mg Hg/g STC in pellet form; the STCP material has shown comparable adsorption over significant periods, i.e. 200 hours, demonstrating an adsorption capacity similar to that of the STC in pellet form). Adsorbed SO_2 could also be photocatalytically oxidized at the STCP surface due to the presence of OH* radicals (55), further extending the time until the STCP adsorption sites are exhausted.

Effect of HCl

Chlorine species are known oxidants (35, 78) and thus a high level of Hg oxidation was expected. Figure 5-5 demonstrates mercury oxidation and removal with 100 ppm_v HCl (all other conditions equal to the baseline) yielding ca. 90% mercury removal, which is a only a slight improvement in Hg removal compared to the baseline, although oxidation increased to almost 99%.

As expected, an air stream with 100 ppm_v HCl and 350 ppm_v SO_2 does not significantly impact STCP performance, as seen in Figure 5-6, where Hg removal is ca. 80-85%. While the chlorine aids oxidation without SO_2 present, it seems the SO_2 is inhibiting Hg oxidation by reacting with HCl in the gas phase, possibly via formation of sulfur-chlorine complexes, thereby reducing the availability of chlorine to oxidize mercury (43, 79). This is confirmed by the lower Hg oxidation in Figure 5-6 as compared to Figure 5-5.

Interestingly, when comparing experiments that contain chlorine with experiments that do not, there is a difference in the time before steady state mercury removal is reached. Figures 5-3 and 5-4 do not include chlorine in the air stream and an increase in mercury removal can be observed before steady state is reached. In contrast, Figures 5-5, 5-6, 5-7, and 5-8 show experiments containing mercury removal, and steady state is reached more quickly. In the absence of chlorine, this lag-effect is likely due to the initial build-up of HgO on the STCP surface, which has a high affinity to elemental mercury, thus facilitating further mercury adsorption (20, 80). The presence of chlorine aids in the oxidation of mercury, overcoming the initial hurdle of forming HgO on the surface.

Effect of Simulated Flue Gas

In Figures 5-7 and 5-8, all constituents were added (NO_2, SO_2, and HCl) at 275°F and 375°F, respectively. Mercury removal did not change significantly compared to the baseline, confirming the resiliency in performance of the coated material to the flue gas constituents tested.

A summary of STCP results is provided in Table 5-1, where removal is given as the steady state mercury removal (in %) across replicate runs. As can be seen in Table

5-2, results were replicable with a good degree of consistency, thus yielding low standard errors across runs.

Summary

A novel photocatalytic silica-titania composite technology was tested under flue gas conditions. Removal rates of 85% were achieved under bench-scale conditions simulating coal combustion flue gas. Temperature did not have a significant effect on removal performance under simulated flue gas conditions. At 375°F, water vapor had a negative effect on mercury removal. By introducing chlorine into the air stream, mercury removal performance improved to levels approximately equal to those at 275°F.

Overall, the technology is promising, but performance might be susceptible to fluctuations in chlorine levels in the flue gas. Research on minimum concentrations of chlorine required to counteract the negative effects of water vapor at high temperatures is necessary for future development as an option for full-scale implementation in coal combustion flue gas environments.

Table 5-1. Summary of results in % mercury removal.

Temp (°F)	No added water vapor	4% RH	4% RH, 250 ppm NO_2	4% RH, 350 ppm SO_2	4% RH, 100 ppm HCl	4% RH, SO_2, HCl	4% RH, NO_2, SO_2,HCl
275	75	80	78.5	80.5	87.5	82	85
375	90	55.5	49	48	89	80.5	84

Table 5-2. Standard error of STCP results in % mercury removal.

Temp (°F)	No added water vapor	4% RH	4% RH, 250 ppm NO_2	4% RH, 350 ppm SO_2	4% RH, 100 ppm HCl	4% RH, SO_2,HCl	4% RH, NO_2, SO_2,HCl
275	0	2	0.5	2.5	0.5	2	1
375	5	1.5	5	2	1	1.5	1

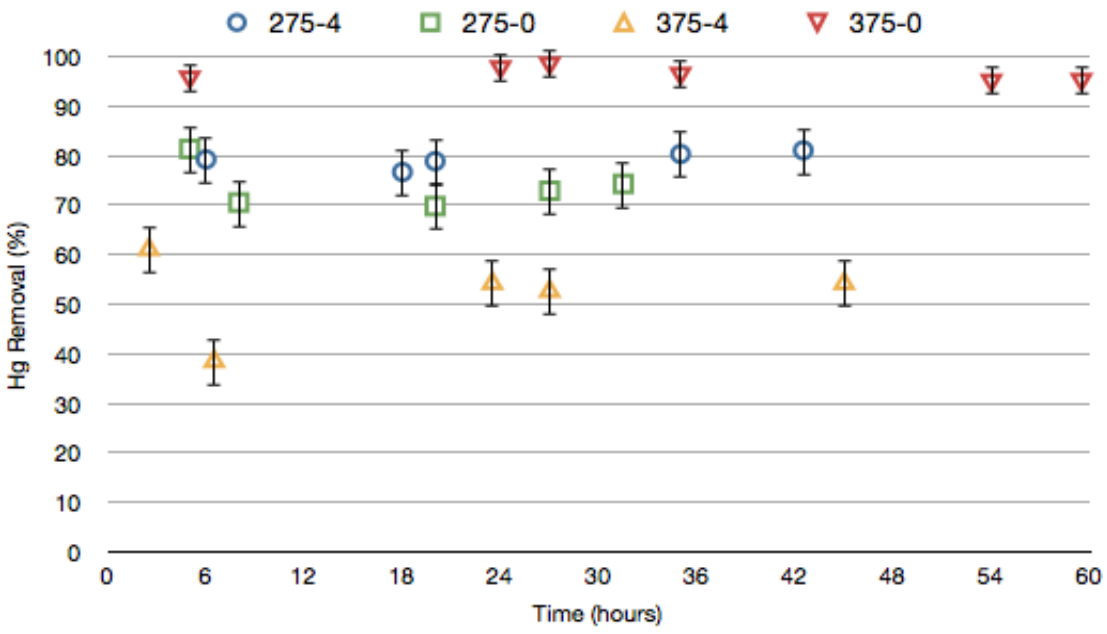

Figure 5-1. Hg oxidation/removal using STCP at 275°F and 43,000 ppm_v WVC.

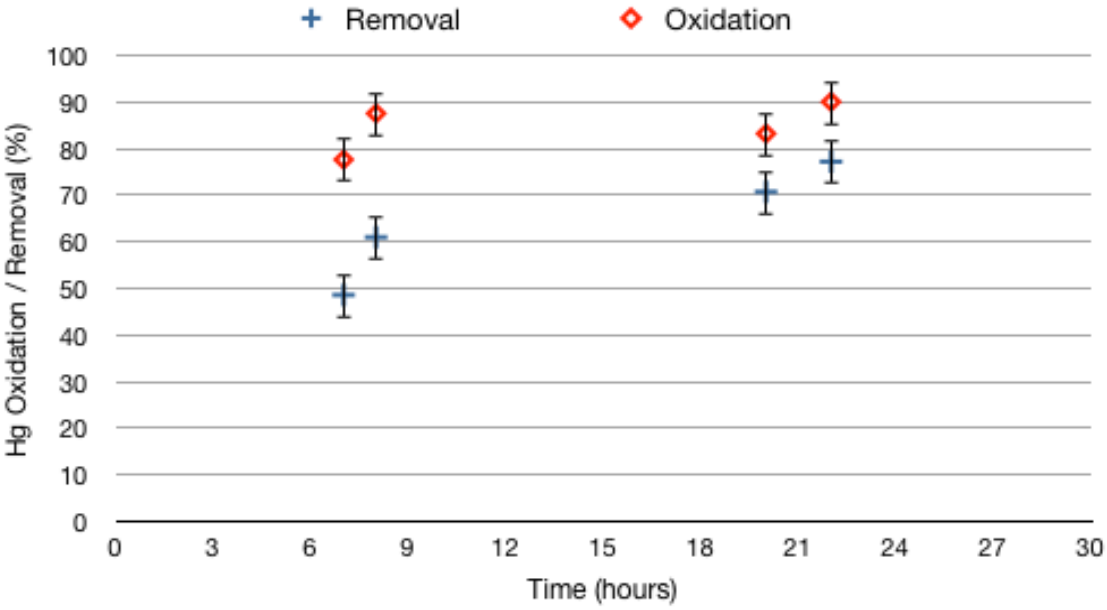

Figure 5-2. Hg oxidation/removal using STCP at 275°F and 43,000 ppm_v WVC, 250 ppm_v NO_2.

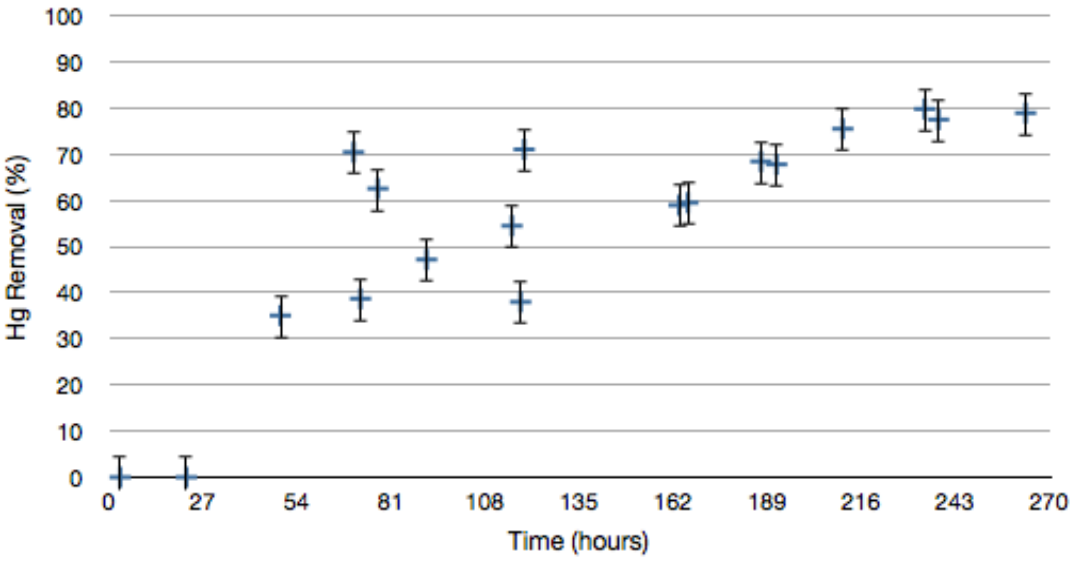

Figure 5-3. Long-term Hg oxidation/removal using STCP at 275°F and 43,000 ppm_v WVC, 250 ppm_v NO_2.

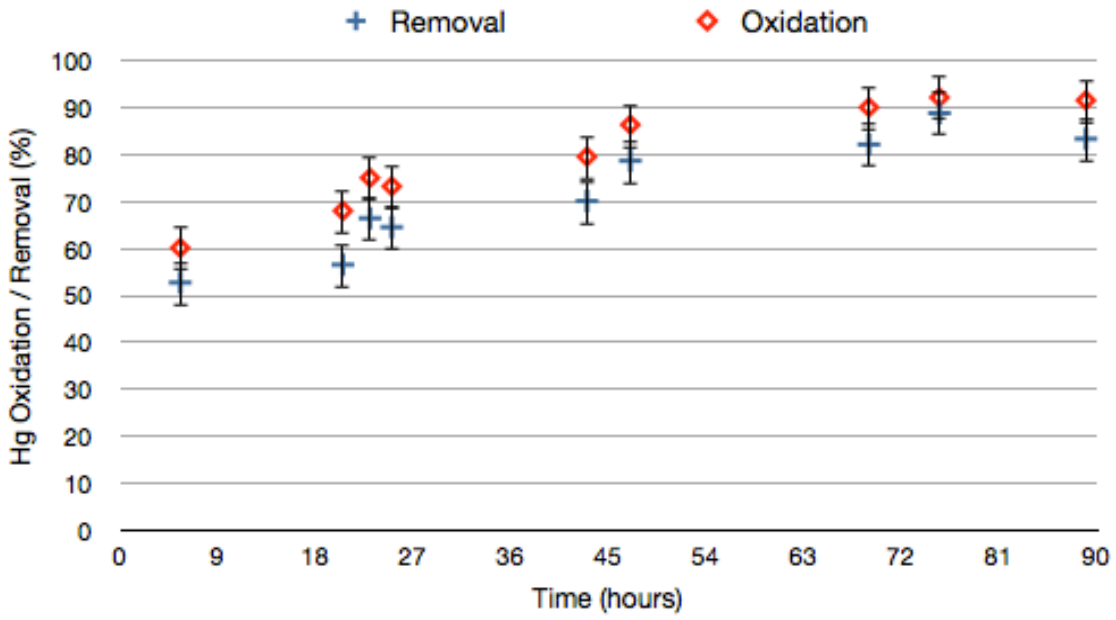

Figure 5-4. Hg oxidation/removal using STCP at 275°F and 43,000 ppm_v WVC, 350 ppm_v SO_2.

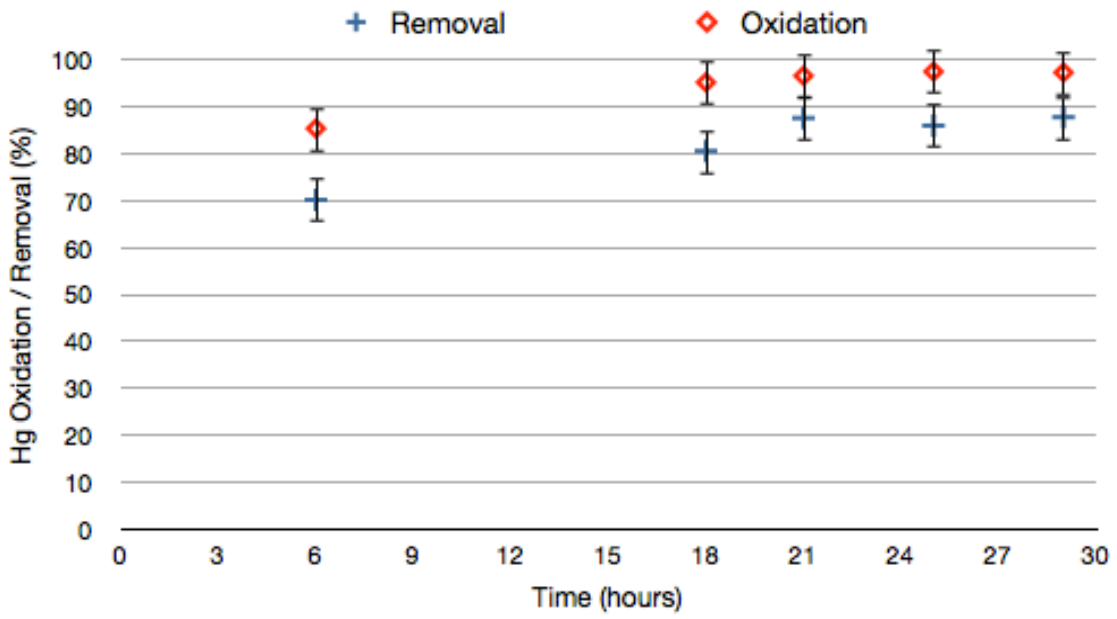

Figure 5-5. Hg oxidation/removal using STCP at 275°F and 43,000 ppm_v WVC, 100 ppm_v HCl.

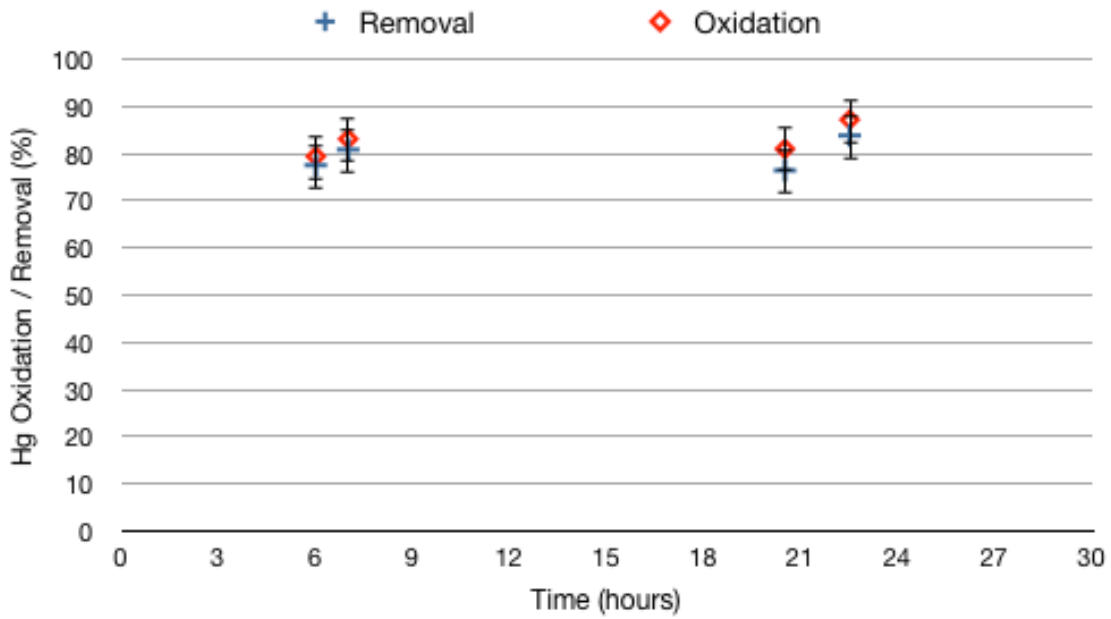

Figure 5-6. Hg oxidation/removal using STCP at 275°F and 43,000 ppm_v WVC, 100 ppm_v HCl, 350 ppm_v SO_2.

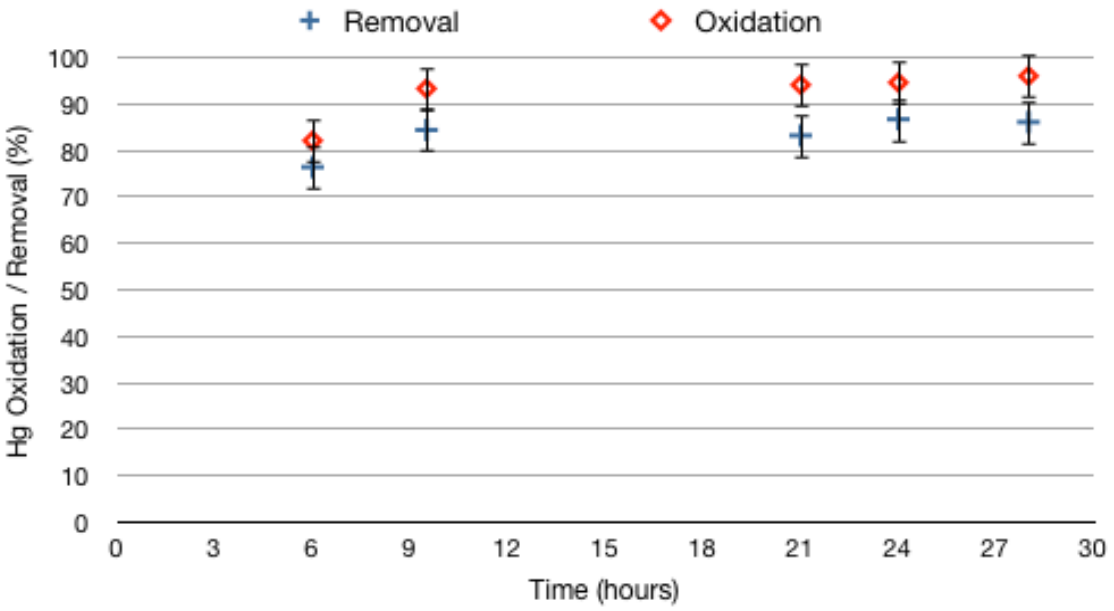

Figure 5-7. Hg oxidation/removal using STCP at 275°F and 43,000 ppm_v WVC, 250 ppm_v NO_2, 100 ppm_v HCl, 350 ppm_v SO_2.

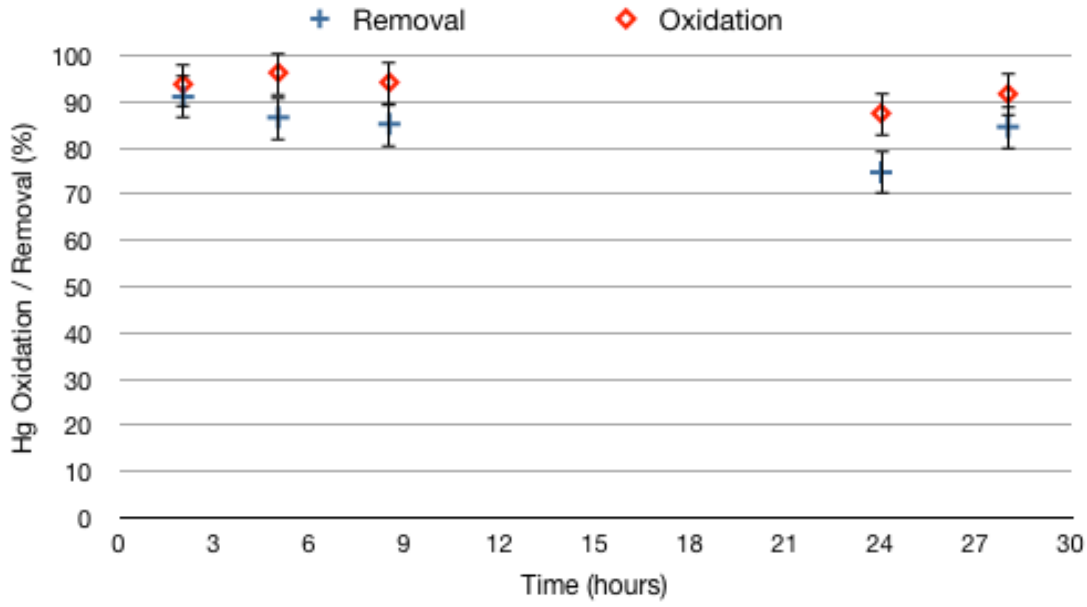

Figure 5-8. Hg oxidation/removal using STCP at 375°F and 197,000 ppm_v WVC, 250 ppm_v NO_2, 100 ppm_v HCl, 350 ppm_v SO_2.

CHAPTER 6
PILOT-SCALE MERCURY REMOVAL USING STCP

An important issue surrounding the use of coal for energy production is the control of hazardous pollutant emissions resulting from combustion. Emissions of mercury (Hg) are of particular concern for existing and proposed coal-fired power plants. Hg is a widespread and persistent pollutant that accumulates in the environment and has contaminated bodies of water worldwide, particularly via deposition from the air. In the US approximately 5% to 10% of women of childbearing age are estimated to exceed federal exposure guidelines due to dietary intake of Hg-contaminated fish (81). This exposure can lead to adverse neurological effects, particularly in the developing fetus and during early childhood. Recently, Hg has been linked to a cause of autism and ADHD in children (82).

Activated carbon injection (ACI) is believed to be the most promising technology for near-term mercury control, but its effectiveness under various conditions is still being investigated (83). Commercially available powdered activated carbon (PAC) has its limitations, resulting in poor Hg removal under certain conditions, unless impregnated with halogens, which substantially adds to cost. PAC is particularly ineffective in removing elemental Hg, and thus will struggle to achieve high levels of Hg removal in conditions where this Hg species is predominant (e.g., when burning lignite or powder river basin (PRB) coal). Although halogenation improves performance in these conditions, the release of halogens from the PAC has led to concerns about corrosion of equipment, emissions of halogens in the flue gas, and impact on the safety and usability of coal combustion by-products (84-86). Additionally, waste PAC accumulates in fly ash, a product of combustion commonly sold for the manufacturing of concrete and

other materials, thus compromising this potential source of revenue generation. The goal of the research presented here was to develop a novel adsorbent packing coated with a silica-titania photocatalyst (herein referred to as Silica-Titania Coated Packing, STCP) that can capture greater than 90% of Hg in flue gas with lower O&M costs than ACI.

An innovative silica-titania composite (STC) material and process for Hg capture has been developed. This technology focuses on the combination of adsorption and photocatalytic oxidation for pollutant removal (25, 51, 80). The STC has demonstrated Hg capture orders of magnitude greater (300 mg/g) than achievable by PAC. Previous research efforts using STC have been completed successfully in the bench scale and in a pilot-scale study at a US chlor-alkali facility (i.e., chemical manufacturing plant), leading to the design, fabrication, and installation of two full-scale commercial units (51).

In the current commercial application, the STC material is employed in a packed bed of STC pellets. A packed bed of STC pellets is well suited for treating flow rates on the order of 2000 ACFM or less, such as those found in the chlor-alkali industry, and when sufficient pressure drop is available. However, when employing the technology for higher flow rates, such as those associated with coal-fired boiler flue gas (greater than 100,000 ACFM), a reactor employing a packed bed of pellets may not be the best solution, since the associated pressure drop may be significant. Recognizing this limitation, we have developed a durable material consisting of commercially available chemical tower packing that is coated with a thin film of STC, to be used in a fixed bed. This STCP has a large external surface area and high void space, which is expected to result in a significantly lower pressure drop (expected to be below 3 to 5 inches of water

gauge (WG) depending on the void space of the packing material and residence time required for greater than 90% Hg capture) than that associated with a packed bed of STC pellets. This is an acceptable pressure drop range for full-scale operations.

The STCP technology would offer the power industry a robust and economical technology that does not negatively impact the balance of plant issues, does not compromise the salability of fly ash, and is capable of adsorbing all species of Hg; particularly the difficult to remove elemental Hg. Hence, the technology has application to all coal-fired power plants, but is particularly well suited for those utilities that burn lignite or sub-bituminous coal (about 45% of the total US coal-fired power plant capacity), which when combusted produce higher concentrations of elemental Hg compared to ionic Hg.

The objectives of this work were to: (1) optimize the design of the STCP to be used in coal-fired power plant applications, (2) characterize the final product, (3) determine the effectiveness of the STCP for Hg removal from simulated flue gas, and (4) evaluate a scaled up version of the STCP in a small pilot reactor and compare the performance to bench-scale results.

Materials and Methods

STCP Material Development

The first step of the research consisted of the selection of commercially available chemical tower packing materials, and the evaluation of coating procedures and formulations. With regards to packing material selection, it was important that the raw material of construction was resistant to high heat (e.g., greater than 200˚F) and retained the coating. The extent of transmission of UV light through a packed bed of the material was also important, and thus was evaluated. This evaluation was carried out

using a system consisting of a series of varying-sized test “boxes” fabricated with Alzack aluminum, which reflects UV light. A 254 nm UV bulb was center-mounted within an Alzack box, and the box was filled with packing. By use of a UV radiometer “looking” through various port-holes on the box sides, intensity of UV radiation passing through the STCP bed was measured.

The second step consisted of coating procedure selection and recipe development. General research on costs associated with various coating methods previously used by the research team, including dip coating, impregnation, and chemical vapor deposition, led to the conclusion that dip coating would result in the lowest cost for full-scale production. Thus this method was evaluated by directly dipping the selected packing in various silica-titania recipes. Various coats were applied as needed (up to 21 coats), with heating to 120˚C for 30 minutes between coats, to obtain a durable coating.

After obtaining successful coatings (i.e., coatings that would not rub off and appeared uniform to the naked eye), two coated materials were selected, characterized for their physical properties via X-Ray Diffraction (XRD), Scanning Electron Microscope (SEM) imaging and durability/hardness testing, and evaluated for Hg removal efficiency from a simulated flue gas under various conditions, as will be discussed below.

Durability testing consisted of using a rotator, whereby a known weight of each sample was placed in a glass vial, rotated at 3 RPM for four hours, and then reweighed after sieving to eliminate any powder produced from attrition of the coating. In addition, ASTM method D3363 (Standard Test Method for Film Hardness by Pencil Test) was used on both PEG and non-PEG coatings. This method consists of using a set of

calibrated drawing leads (i.e., pencils of different hardness) to attempt to scratch or cut a coating surface by applying pressure with the pencil at a 45˚ angle.

Evaluation of Mercury Removal

This task involved the utilization of a lab-scale test bed (Figure 6-1) with simulated flue gas. The reactor system included a supply of elemental mercury vapor, a mercury analyzer (Ohio Lumex® Zeeman RA-915+), and appropriate appurtenances for measuring total Hg (i.e., elemental and oxidized Hg) via an analogous version of the Ontario Hydro Method (ASTM D6784-02). This modified version skips steps related to particulate matter, as there is no particulate matter present in this simulated flue gas. Hg-laden air was introduced into the annular test reactor by passing nitrogen gas above liquid Hg in a reservoir. The test reactor contained an influent and effluent port and a UV lamp (254 nm, 12 W) encased by a quartz sleeve centered in its annulus. The reactor was randomly packed with STCP. Simulated flue gas containing varying concentrations of Hg, HCl, SO_2, NO_2, air, and water vapor was passed through the packed reactor. Concentrations were controlled by varying flows with flow meters as presented in Figure 6-1. In the case of water vapor and HCl concentrations, these were controlled by the flow of a dilute HCl solution from a 4-liter pressure vessel. Contact time was varied by adjusting the flow of carrier air and/or volume of STCP in the reactor (from 3 to 6 LPM). Temperature was varied and controlled via heat tape surrounding the gas feed lines and the reactor.

The parameters controlled and verified included: (a) inlet and outlet total Hg concentrations measured using the online Hg analyzer and the Ontario Hydro Method for the duration of 24-hour tests, (b) volumetric flow rate of air, (c) flow/concentration of

various “typical” flue gas constituents, and (d) temperatures on the inlet and outlet controlled by heat tape and monitored by thermocouples.

Scaled-Up Evaluation of Mercury Removal from Simulated Flue Gas Using STCP

A 4 ACFM (113 LPM) pilot reactor (schematic shown in Figure 6-2) was built and evaluated in our laboratory using simulated flue gas and the optimal conditions determined in bench-scale evaluations. Various flue gas constituents were added in the same way they were added in the bench-scale experiments described above. Data analyses were also carried out as above.

The reactor design was slightly different than the bench-scale reactor design. The bench-scale reactors were annular, with a quartz sleeve centered in the annulus where a UV lamp is housed. The STCP material was packed around the quartz sleeve, and the test gas flowed upwards through the bed. The 4 ACFM pilot-scale reactor consisted of two sections. The first section was a circular quartz tube. The lamp was placed outside of the quartz tube, and the test gas flowed on the inside of the tube. The second section, downstream of the quartz/UV section, consisted of a ceramic honeycomb coated with the same recipe selected for small bench-scale experiments. Preliminarily, this design was chosen with full-scale commercialization in mind. The hypothesis was that a UV section without STCP could begin the oxidation of Hg while a slightly irradiated STCP section would “complete” the oxidation and remove the oxidized Hg. As proven later, this design was not ideal.

Results and Discussion

STCP Material Development

The first step consisted of selecting the appropriate packing material based on temperature resistance (as indicated by manufacturer specifications) and UV

transmission through the packed bed. Thus the transmission of UV through a packed bed of various uncoated packing materials was evaluated using the Alzack test system described above. Results are summarized in Figure 6-3 and include transmission through a packed bed of STC pellets for comparison. There is better penetration through a packed bed of all packing materials when compared to penetration through the bed of STC, due to the higher void space of the packing. This will not only result in lower UV requirements in a full-scale system, but also result in a lower pressure drop compared to a bed of pellets. Thus any of the tested materials would be better suited than the STC pellets for this application based on UV penetration characteristics (at lamp spacing below 2 inches).

Based on temperature resistance characteristics, three materials were coated: (1) metal rings (Jaeger metal Raschig super rings, 50 mm, 98% void space), (2) 1" Koch-Knight HPC high porosity carrier saddle (67% void space), and (3) 1" LPD® KNIGHT-CHEM® Chemical Porcelain Packing (67% void space). However, the only material that was successfully coated was the Chemical Porcelain Packing, whereas all others resulted in coatings that could be easily wiped off and/or were uneven regardless of coating formulation.

Packing materials were initially dip coated with powdered STC pellets suspended in a solvent and heated (to 120˚C) between coats for 30 minutes to evaporate the solvent. However, these coatings easily rubbed off, and thus other coating recipes were developed (Table 6-1). These included various ratios of TiO_2 (Degussa P25 and also titanium (IV) tetraisopropoxide (TTIP) used as a precursor) to water, plus an added silica source (Ludox colloidal silica). In addition, various additives were included that

were expected to improve the coating quality (e.g., polyethylene glycol (PEG), methylcellulose, and powdered dispersible alumina (Dispal, Disperal)).

STCP Material Characterization

As Table 6-1 indicates, successful coatings were achieved with a combination of a 50% Ludox solution with 3.5% TiO_2 (Degussa P25), with and without PEG. PEG coatings were successful with and without sonication. Since sonication would only lead to a higher energy requirement for material synthesis (and hence higher manufacturing cost), this was not included in the ultimately selected coating strategy.

To analyze the impact of PEG on coating characteristics, two coating methods were characterized: (1) 3.5% TiO_2, 50% Ludox, 50% water (hereon “non-PEG”) and (2) 1% PEG, 3.5% TiO_2, 50% Ludox, not sonicated (hereon “PEG”). The following analyses were carried out: (a) XRD, (b) SEM imaging: of both coatings plus imaging of STCP that had been used in simulated flue gas studies described ahead (hereon “used”), (c) hardness/durability testing, (d) average pore size, (e) average pore volume, and (f) BET surface area. Results are summarized below.

XRD

XRD analyses to determine the ratio of anatase to rutile phase titania were originally proposed assuming there would be successful coatings using various titania precursors. However, the only successful coatings used Degussa P25 as the titania source, which has a known crystalline structure (4:1 anatase to rutile ratio). The analyses were completed and verified that there was a ratio of anatase to rutile that was greater than 1 for three coated samples (PEG, non-PEG, and used).

SEM Imaging

In the PEG sample (Figure 6-4), the deposition of coating is uneven, with layering. Most of the surface appears to be composed of platelets lying flat, but with small quantities of amorphous deposits. The platelets are non-crystalline, probably resulting from cracking of the surface as the layers dried. The nano-porosity of the surface cannot be determined at these magnifications, but most of the platelet surface area is readily accessible. Cracking of platelets during drying provides very limited access to the internal structure on surfaces perpendicular to the faces.

In the non-PEG sample (Figure 6-5), the surface is again composed of layered platelets. However, around 10-20% of the surface area of the plates is covered by a thin layer of amorphous globules. The deposition pattern suggests flow of liquid on the surface, with rapid precipitation of solids during drying, which would not allow effective controlled growth patterns to develop. Whether or not the globules are interspersed between sequential layers of platelets cannot be determined from the available images.

In the “used” sample (Figure 6-6), the “used” surface has substantial deposition of materials of form inconsistent with the virgin surface. Some of the new deposits appear to be crystalline. Some of them form clusters of platelets growing skew or perpendicular to the underlying surface, while others form stacks of smaller platelets (upper right corner).

Hardness/Durability

The durability of the PEG and non-PEG STCP were compared to that of STC pellets and “uncoated” ceramic tower packing. Results are summarized in Table 6-2. As the table indicates, there was a minimal amount of attrition during the rotation period in all cases, with the maximum attrition observed for the Non-PEG sample.

ASTM method D3363 (Standard Test Method for Film Hardness by Pencil Test) was used on both PEG and non-PEG coatings to determine film hardness. The test resulted in Gouge Hardness and Scratch Hardness of 6H for both the PEG and non-PEG coatings. This means that the hardest pencil tested did not scratch or cut either surface.

Pore size, pore volume, and surface area

The PEG and non-PEG samples were analyzed for pore size, pore volume, and surface area. The results can be found in Table 6-3.

Simulated Flue Gas Bench-scale Experiments

Because the PEG and non-PEG coated materials had similar characteristics, it was decided to carry out the majority of bench-scale evaluations using the non-PEG material. Based on preliminary work carried out with STC pellets, at least a 1 s contact time was required for high temperature, high relative humidity applications such as the coal-fired power plant flue gas application of interest here (e.g., lignite-fired boiler). Thus, initial testing of the non-PEG material was initiated with a 2 s contact time.

Through discussions with a lignite-fired electric utility, test conditions were established to represent those of where the technology could be applied. These included 375˚F, 350 ppm_v of SO_2, 250 ppm_v of NO_x, and 100 ppm_v of HCl. Before testing these collectively, tests were performed without the presence of sulfur, NO_x, and chlorine.

In general, oxidation was very high throughout the 24-hour period, and removal was greater than 90% for the majority of the duration, with a slight decrease to 87% in the final data point.

Because different utilities will exhibit different flue gas temperatures and relative humidities, the testing environment was challenged by adding 4% relative humidity to the feed. In addition, as flue gas will have varying amounts of chloride present (depending on type of coal burned), HCl (100 ppm_v) was incorporated into the simulated flue gas stream. Results are shown in Figure 6-8. It should be pointed out that 100 ppm_v HCl is a relatively low concentration for flue gas. There was no significant difference in oxidation/removal when comparing Figure 6-7 to Figure 6-8.

Sulfur compounds are known to negatively impact the performance of activated carbon. In flue gas conditions particularly, the presence of SO_2/SO_3 will be a challenge for activated carbon. Thus, SO_2 (350 ppm_v) was incorporated into the flue gas stream next to determine its effect on the STCP performance.

As shown in Figure 6-9, excellent oxidation (92 – 99%) and removal (86 – 97%) were obtained when adding the challenging SO_2 to the simulated flue gas stream. While the data appears to drop off, it is expected to remain steady above 80% for extended periods based on previous testing not discussed here. It should be pointed out that past studies with STC pellets have shown similar results with SO_2 concentrations as high as 3500 ppm_v. Ahead it will be demonstrated that STC pellets and STCP perform very similarly, if not identically, under the conditions evaluated here.

Nitrogen compounds are abundant in flue gas conditions, and may negatively impact some technologies, such as activated carbon. Thus, NO_2 was incorporated into the simulated flue gas stream to determine its effect on the STCP performance. As Figure 6-10 indicates, NO_2 does not negatively impact performance of the STCP. Oxidation ranged from 92 to 100% and removal ranged from 91 to 93%.

In order to directly compare between the performance of the STCP and the STC, the work presented in Figure 6-10 was repeated under the same conditions (i.e., contact time, temperature, constituent concentration, and relative humidity), but using STC pellets rather than STCP. Results are summarized in Figure 6-11. As the Figure indicates, oxidation ranged from 92 to 100% and removal ranged from 89 to 99%. Although at times removal was higher than that observed with the STCP, performance is very similar.

In order to attempt to decrease the 2 s contact time used for most of the experiments summarized above, a final run was completed at 375˚F with 4% relative humidity, 10 ppb Hg, 100 ppm_v HCl, 350 ppm_v SO_2, and 250 ppm_v NO_2 but with a 1 s contact time.

As Figure 6-12 shows, oxidation varied from 90 to 97% and removal varied from 72 to 78%. This is a decline in removal when compared to that obtained with a 2 s contact time (Figure 6-11).

4 ACFM Pilot-Scale Data

To evaluate the scale-up potential of the STCP technology, a few experiments were carried out using a 4 ACFM (113 LPM) pilot reactor designed and fabricated for this purpose. The first experiment was carried out at 375˚F (191˚C), with 4% relative humidity and no added additional constituents, other than 100 ppm_v HCl. The second was carried out at 200˚F (93˚C), with 4% relative humidity and no added additional constituents, other than 100 ppm_v HCl. The second conditions were examined since the lower temperature is representative of flue gas after a wet scrubber, for example. As Figure 6-13 indicates, oxidation ranged from 70 to 76% and removal from 45 to 59% at 375˚F, whereas at 200˚F oxidation ranged from 89 to 91% and removal from 67 to

74%. This difference in performance when compared to bench-scale tests is attributed to the difference in design. In the bench-scale reactor design, the STCP is in direct contact with the UV lamp encased in a quartz sleeve. In the small pilot-scale reactor, the only direct UV/STCP contact occurs on the interface of the two sections described earlier (UV section followed by honeycomb section). Although it is known that 254 nm UV will oxidize elemental Hg, clearly the oxidation ability is much lower at 375˚F (70 - 76%) than that observed when incorporating UV plus STCP (greater than 90%). It is expected that a scaled up design with more irradiation of the STCP will result in greater oxidation and removal.

Competitive Analysis

Table 6-4 includes a summary of characteristics and costs of the STCP in comparison two of the most widely accepted technologies for Hg removal from coal-fired utility flue gas. Cost estimates, which factor in capital and O&M costs, are based on a ten-year cost analysis.

Summary

A durable and even silica-titania coating can be obtained by dip coating ceramic chemical tower packing in a 3.5% TiO_2, 50% Ludox (in water) solution. This coated packing, termed STCP, is as effective as the previously developed STC in oxidizing and removing Hg from simulated flue gas, resulting in greater than 90% oxidation and removal in conditions “typical” of various flue gases from electric utilities. Flue gas components that generally affect performance with other technologies, such as ACI, did not negatively impact the STCP’s Hg oxidation and removal efficiency. A 2-second contact time was the optimum determined in this study, which certainly leaves room for optimization.

A major concern of most technologies considered for Hg control in coal-fired power plants is the effect of temperature. The data collected here at 375˚F is very promising, particularly because this temperature is in the upper range of temperatures expected in flue gas. A second concern is the fact that sulfur species poison most catalysts and sorbents. The data presented here would indicate that SO_2 does not have a negative impact on performance.

Table 6-1. Coating recipes that were attempted during this study.

"Good" coating recipes	"Bad" coating recipes
	STC suspension
1% PEG, 3.5% TiO_2, 50% Ludox, sonicated	0.1% TiO_2, water, sonicated
3.5% TiO_2, 50% Ludox, 50% water	7% TiO_2, water, sonicated
1% PEG, 3.5% TiO_2, 50% Ludox, not sonicated	1% TiO_2, sonicated
	7% TiO_2, washed before coating
	1% TiO_2, washed
	1% PEG, 3.5% TiO_2, water, sonicated
	25/75 high surface area TiO_2, water, TiO_2
	3.5% TiO_2, 100% Ludox
	3.5% TiO_2, 3.5% Dispal (alumina powder), water
	3.5% TiO_2, 3.5% Disperal (alumina powder), 50% water, 50% Ludox
	1% methylcellulose, 3.5% TiO_2, 50% Ludox, 50% water
	1% methylcellulose, 3.5% TiO_2, 100% water
	TTIP (titania precursor)/Degussa 0.5M
	TTIP 0.5M

Table 6-2. Summary of durability test results.

Type	Starting Mass (g)	Post Rotating Mass (g)	Mass Loss (g)	% Mass Loss
Uncoated Ceramic	30.01	30.01	0	0%
STC	30.051	29.9884	0.0626	0.21%
PEG	30.14	30.07	0.07	0.23%
Non-PEG	30.02	29.89	0.13	0.43%

Table 6-3. Characteristics of PEG and non-PEG packing.

Material - Parameter	Avg. pore size (Å)	Pore volume (cc/g)	BET surface area (m^2/g)
PEG	82.4	0.0234	11.4
Non-PEG	73.3	0.0204	11.2

Table 6-4. Competitive analysis of STCP versus two widely accepted commercial technologies for Hg removal from flue gas.

Technology	Silica-Titania Coated Packing	Activated Carbon Injection	TOXECON
Removes Hg	YES	Only if oxidized	Only if oxidized
Oxidizes Hg	YES	Only if halogen (e.g., bromine) present	Only if halogen (e.g., bromine) present
Unaffected by Sulfur	YES	NO	NO
Operation	Packed Bed	Injection/Removal	Injection/Removal
Material Life	Estimated at 10 yrs	Single-use	Single-use
Maintains Fly Ash Salability	YES	NO	YES
Average Annual Cost ($/year)	3,350	27,000	20,000

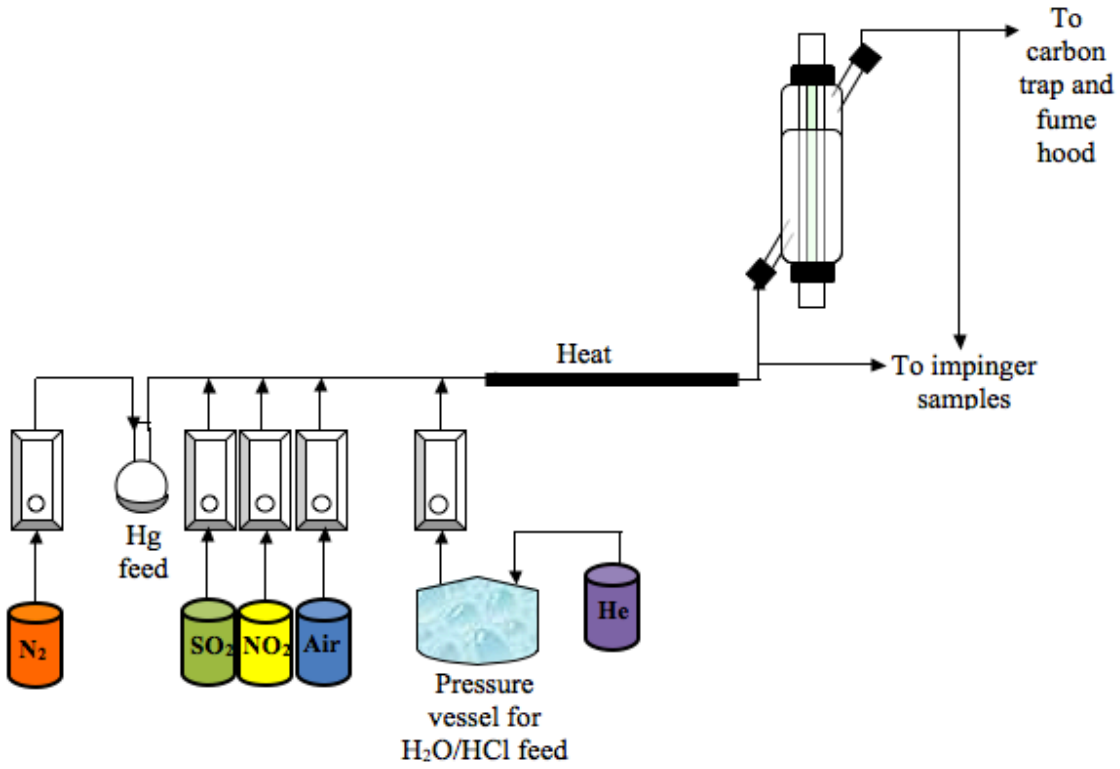

Figure 6-1. Test stand schematic for bench-scale studies for evaluation of STCP for Hg removal from simulated flue gas.

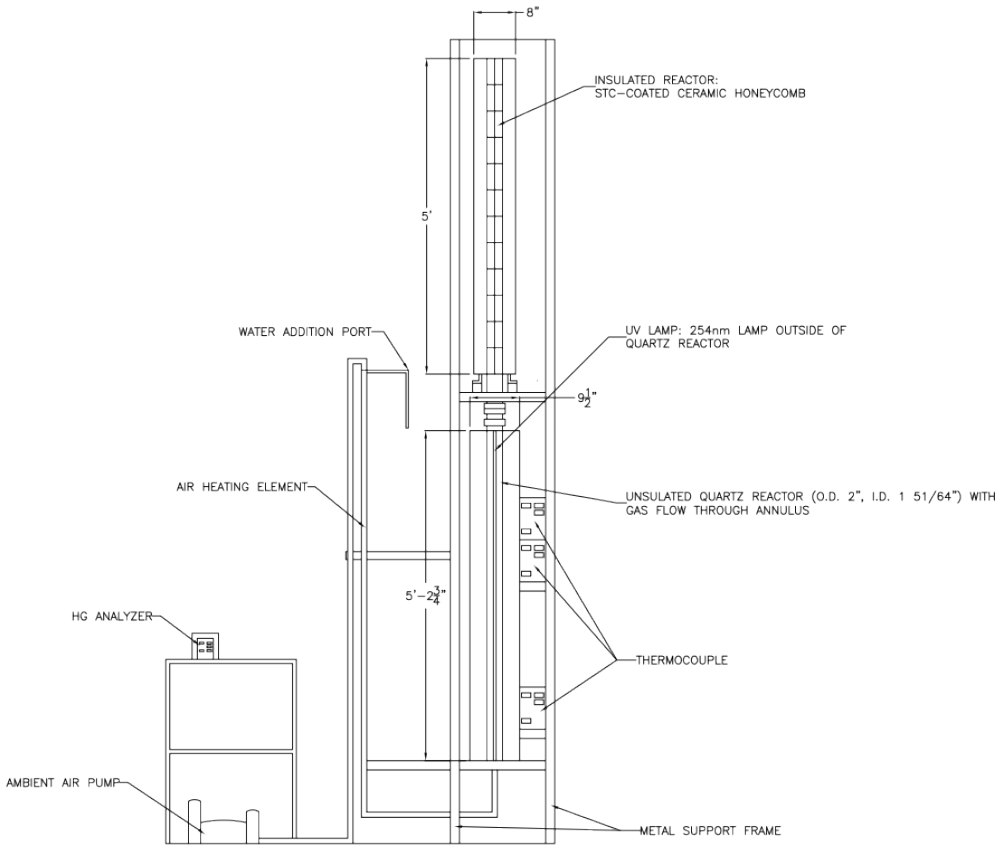

Figure 6-2. Schematic of 4 ACFM pilot-scale reactor used for scaled-up evaluation of STCP for Hg removal from simulated flue gas.

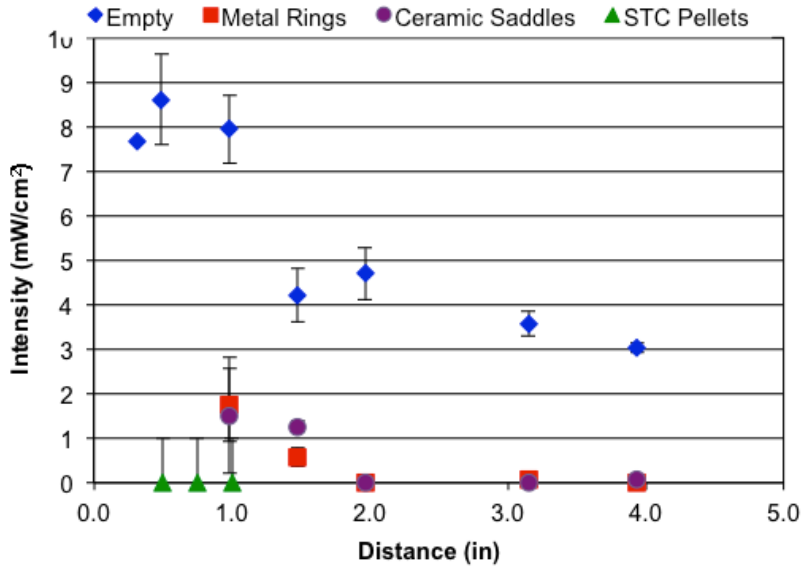

Figure 6-3. UV transmission through a packed bed of various materials.

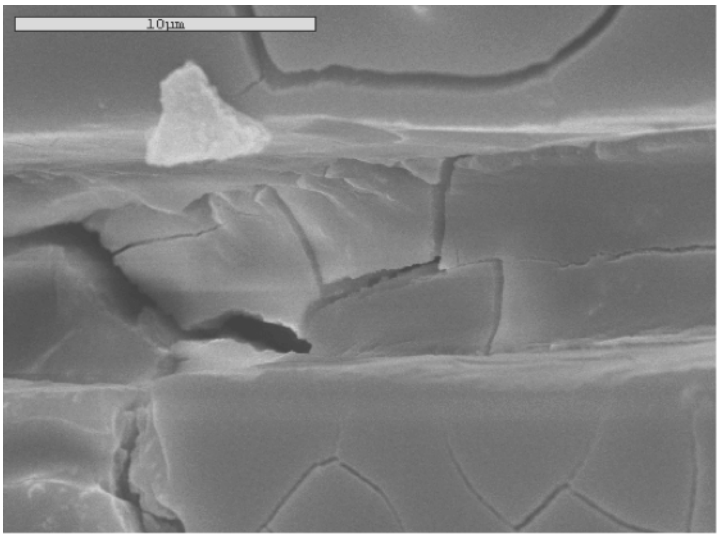

Figure 6-4. SEM imaging of PEG packing (5000X magnification).

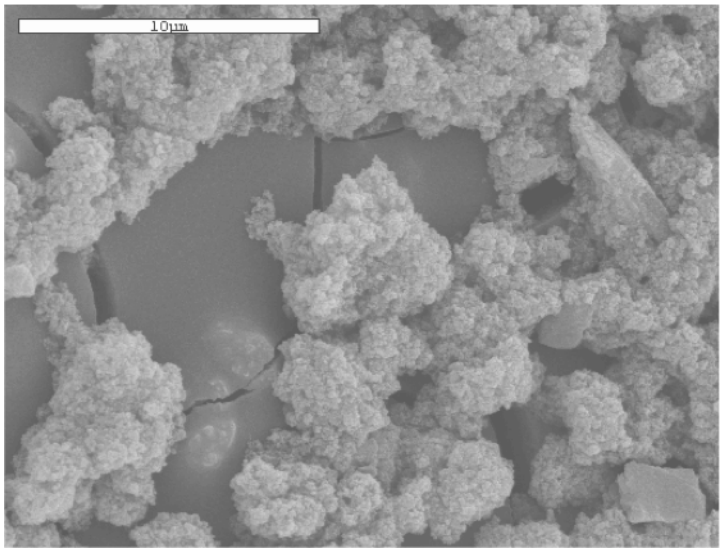

Figure 6-5. SEM imaging of non-PEG packing (5,000X magnification).

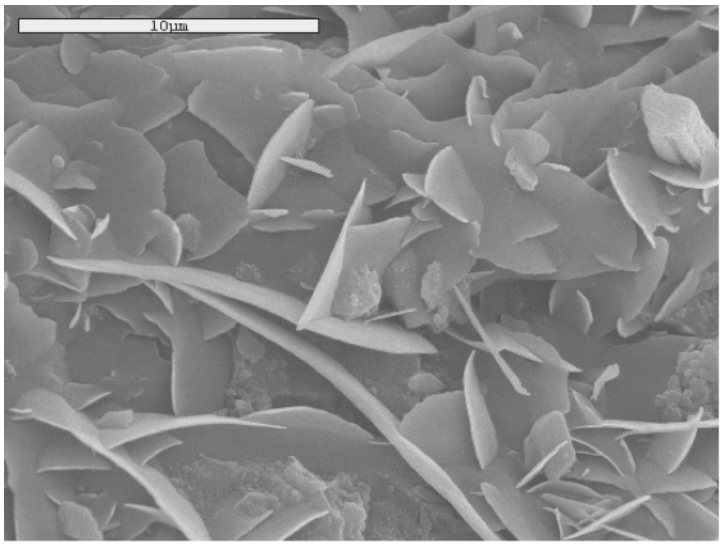

Figure 6-6. SEM imaging of used packing (5,000X magnification).

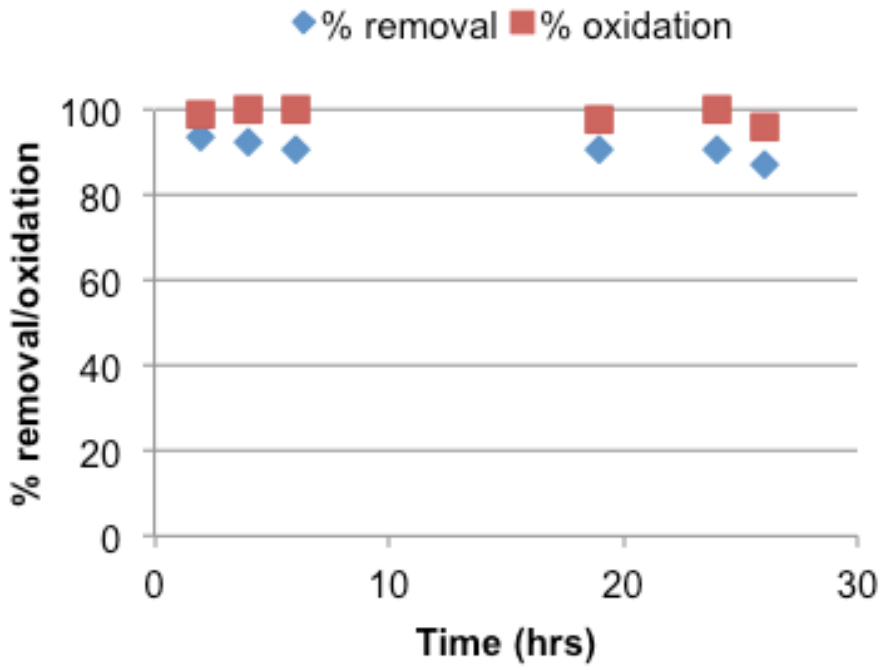

Figure 6-7. 375˚F, 2 s contact time, 10 ppb Hg, no added humidity, non-PEG STCP.

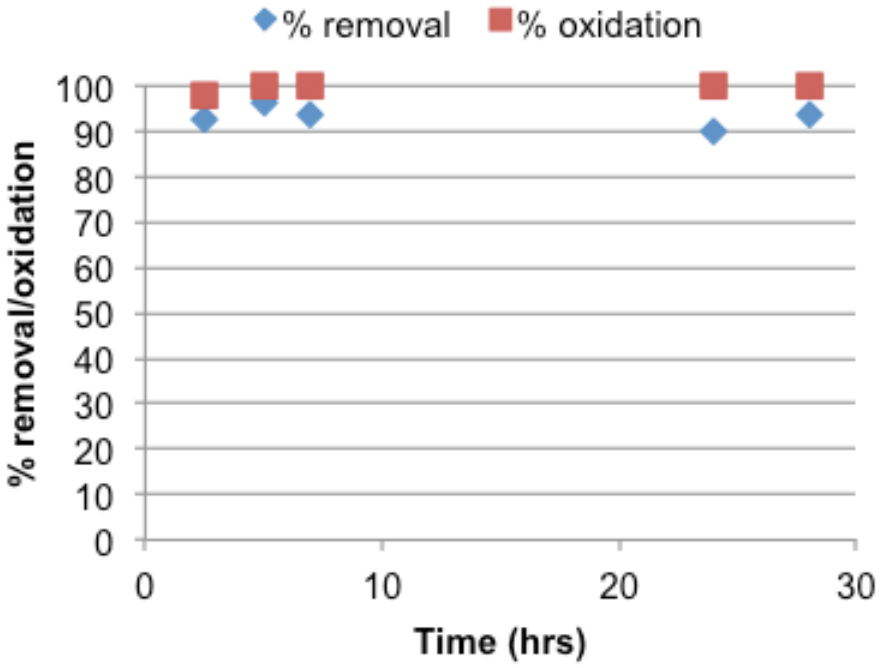

Figure 6-8. 375˚F, 2 s contact time, 10 ppb Hg, 4% relative humidity, non-PEG STCP, 100 ppm HCl.

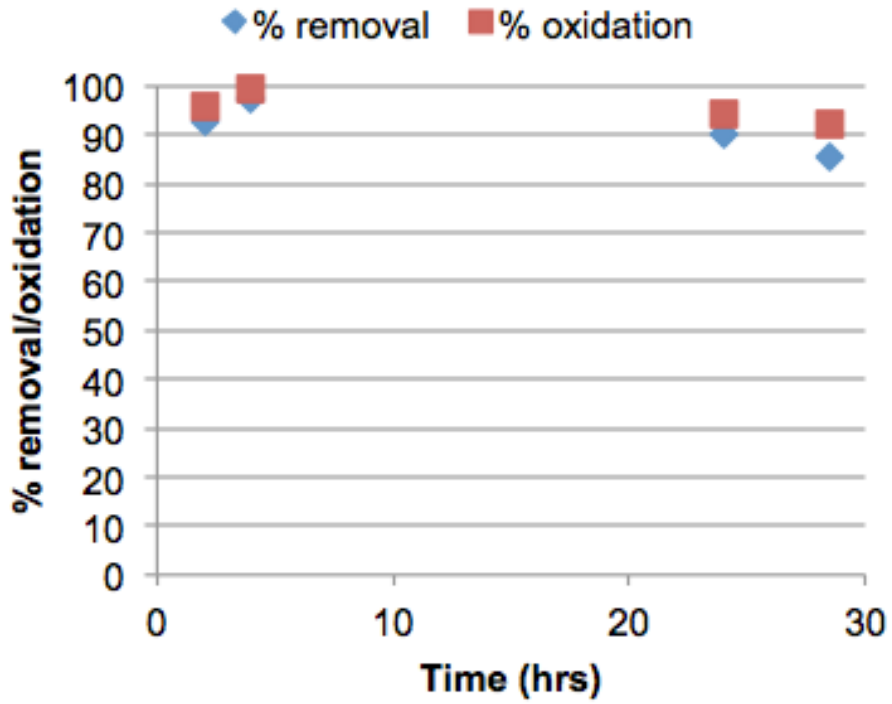

Figure 6-9. 375˚F, 2 s contact time, 10 ppb Hg, 4% relative humidity, non-PEG STCP, 100 ppm HCl, 350 ppm SO_2.

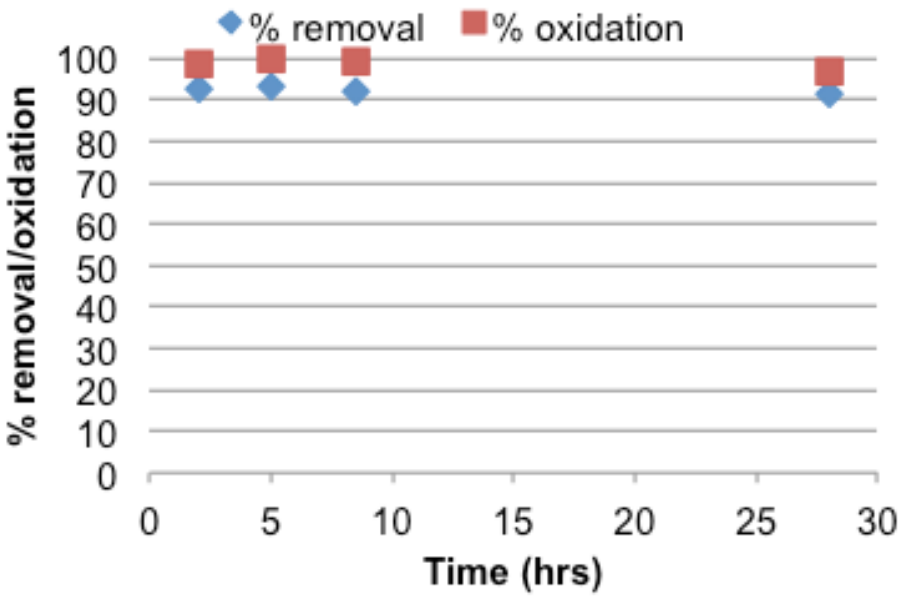

Figure 6-10. 375˚F, 2 s contact time, 10 ppb Hg, 4% relative humidity, non-PEG STCP, 100 ppm HCl, 350 ppm SO_2, 250 ppm NO_2.

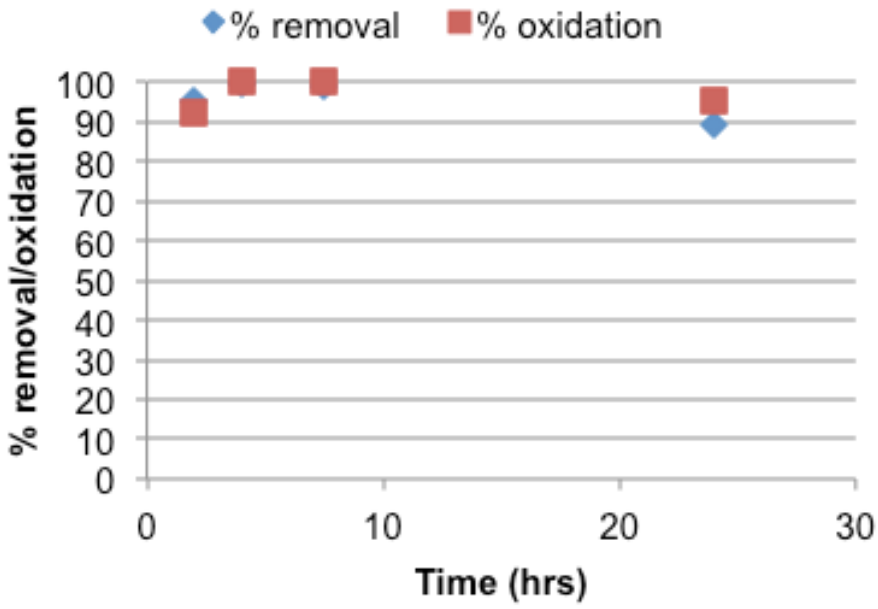

Figure 6-11. 375˚F, 2 s contact time, 10 ppb Hg, 4% relative humidity, 100 ppm HCl, 350 ppm SO_2, 250 ppm NO_2. Media: 3 mm by 5 mm cylindrical STC pellets (140Å pore size, 12% TiO_2).

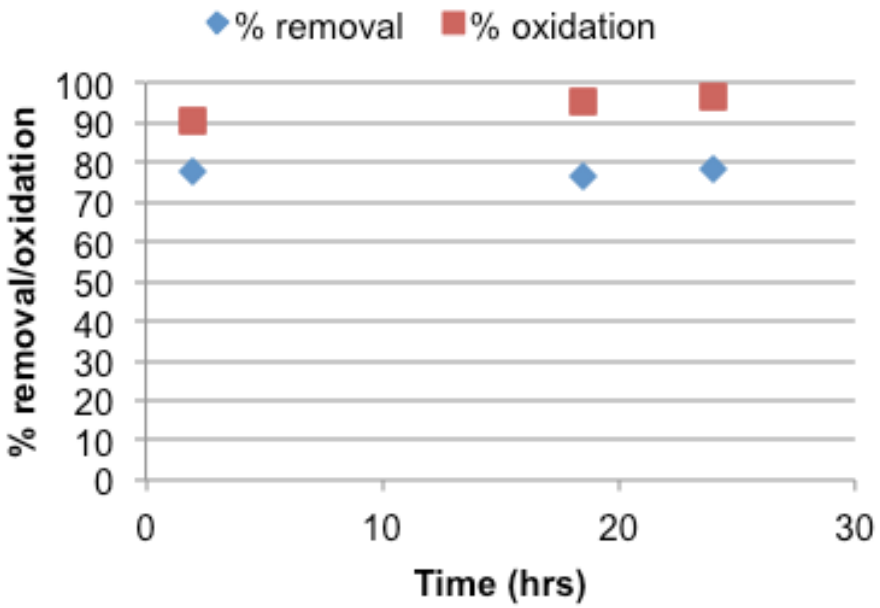

Figure 6-12. 375˚F, 1 s contact time, 10 ppb Hg, 4% relative humidity, non-PEG STCP, 100 ppm HCl, 350 ppm SO_2, 250 ppm NO_2.

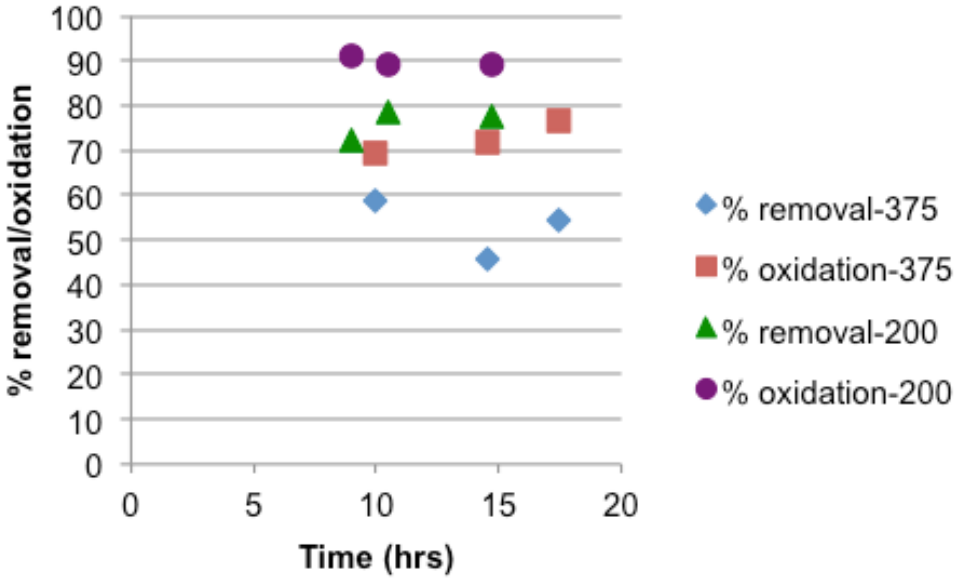

Figure 6-13. Results of 4 ACFM pilot-scale evaluation of non-PEG coated honeycomb at the following conditions: 375 or 200˚F, 1.2 s contact time in each of two sections defined earlier, 10 ppb Hg, 4% relative humidity, and 100 ppm HCl.

CHAPTER 7
CONCLUSIONS

Mercury oxidation by UV was studied at three UV wavelengths (365 nm, 254 nm and 185 nm) over a range of water vapor concentrations. Oxidation was higher with the 185 nm over the range of temperatures and water vapor concentrations than 254 nm. No mercury oxidation was detectable with the 365 nm bulb in any conditions. While lack of water vapor seemed to inhibit oxidation at the 254 nm wavelength, oxidation increased as water vapor concentration was increased. UV irradiation at 185 nm was steadier over the range of water vapor concentrations tested. As water vapor concentration was further increased, mercury oxidation seemed to be slightly inhibited under most test conditions. Based on its ability to oxidize mercury under conditions with a limited amount of water vapor present this method is capable of removing mercury in conjunction with a capturing mechanism, such as a wet FGD scrubber, under certain conditions.

The STCP material built on the STC technology to optimize pressure drop across the treatment system of a coal combustion flue gas. Chemical tower packing material was coated with a silica-titania suspension. Removal rates of 85% were achieved under bench-scale conditions simulating coal combustion flue gas. Temperature did not have a significant effect on removal performance under simulated flue gas conditions. At 375°F, water vapor had a negative effect on mercury removal. By introducing chlorine into the air stream, mercury removal performance improved to levels approximately equal to those at 275°F. Overall, the technology is promising, but performance might be susceptible to fluctuations in chlorine levels in the flue gas. It is also promising that performance at 375°F under simulated flue gas conditions is still

high, as that temperature is in the upper range of temperatures expected in flue gas. Finally, the data presented here indicates that SO_2 does not have a negative impact on performance, which is a drawback of other technologies employing catalysts.

Air-phase VOC removal using STC pellets under UV irradiation was studied for application in aircraft cabin air purification. Pellets were smaller than in previous work involving STC in order to increase surface area of the STC material. The effectiveness of the STC technology for removal of VOCs for application in aircraft cabin air purification was successfully demonstrated, as it was able to effectively remove toluene and ethanol via adsorption alone. Regeneration with 254 nm UV plus sweep air was proven effective for average flight lengths (i.e., 4 hours). When using ethanol as the target pollutant, regeneration with 254 nm UV plus sweep air was proven effective for long haul flights, which indicates it would also be effective for shorter flights.

The STC technology overcomes the limitations of typical PCO systems (constant irradiation, poor mass transfer). The high surface area adsorbent also allows for the preferred operation of adsorption during flight and regeneration between flights. This mode of operation would not only achieve high levels of contaminant removal, but would also eliminate the possibility of releasing toxic intermediate oxidation by-products into the air during flight.

The STC/STCP material, both in pellet and coated forms, was successfully applied to both organic and inorganic pollutant control under various conditions. For application in both coal combustion flue gas mercury removal and aircraft cabin air purification, the fundamental silica-titania photocatalytic technology was adapted to fit the environmental conditions and shown to be technologically feasible.

Recommendations for future work are listed below:

- Further investigation of water vapor interaction with STCP surface.
- Characterization of used STCP with environmental SEM.
- Further development of the STC technology for application in VOC treatment using a larger reactor and LED UV for improved energy efficiency.

This work has made the following contributions to science:

- First to study oxidation of elemental mercury by UV alone at wavelengths of 254 nm and 185 nm at various temperatures and moisture levels.
- Developed STCP material as an improvement on the limitations of STC in pellet form, in particular the issue of pressure drop.
- Characterization of STCP material by XRD, SEM and nitrogen adsorption isotherm.
- Demonstrated the efficacy of the STCP material under bench-scale and pilot-scale simulated flue gas conditions at higher temperatures than in previous research.
- Demonstrated removal of VOCs (specifically toluene and ethanol) by STC pellets under UV irradiation.

APPENDIX
VOC REMOVAL BY STC PELLETS

Volatile organic compounds (VOCs) are among the most abundant chemical compounds in indoor air, including aircraft cabin air, and may negatively impact human health. In fact, negative health effects experienced by pilots and flight crews have led to numerous studies on what is termed “aerotoxic syndrome” (87). Symptoms of aerotoxic syndrome include headache, eye and nose irritation, cough, shortness of breath, chest tightness, increased heart rate, light-headedness, dizziness, blurred or tunnel vision, disorientation, confusion, memory impairment, shaking and tremors, loss of balance, vertigo, nausea, vomiting, seizures, and loss of consciousness.

The airline and its support industry have been focused on the development of solutions that are more effective than traditional activated carbon filters, which must be replaced regularly when they reach their adsorption capacity. One promising solution is photocatalytic oxidation (PCO), which results in the chemical destruction of VOCs, but the concerns surrounding intermediate by-products from incomplete oxidation have prevented this technology from being implemented (88). A high surface area sorbent and photocatalyst, STC is used in this study, which has been previously evaluated for removal of VOCs and hazardous air pollutants (HAPs) from gases emitted from pulp and paper mills (50, 89, 90), removal of synthetic organic compounds from gray water (91-93), mercury removal from flue gas (19, 25, 80), mercury removal from caustic exhaust at chlor-alkali facilities (51), and pathogen deactivation (94). Due to the unique characteristics of the STC, the technology can be used to adsorb VOCs during flight (without UV), with regeneration (UV irradiation for destruction of sorbed VOCs) on the tarmac while the aircraft is prepared for its next voyage. A small volume of recirculated

sweep air may assist with regeneration, followed by exhausting to the atmosphere. In this manner, passengers and flight crews would be protected during flight, and if problematic intermediates are developed during regeneration, they can be vented to the atmosphere or to an on-the-tarmac adsorbent bed. Complete "mineralization" of adsorbed VOCs to water and carbon dioxide during regeneration is the desired goal, to avoid any venting of VOCs. Although initial research presented here has focused on the development of the STC for aircraft cabin air purification, the technology can be extended for use in air revitalization and odor control in space exploration vehicles and architectures. Additionally, a PCO system as described herein could contribute to the design of heating ventilation and air conditioning (HVAC) systems with lower energy requirements, resulting in significant energy savings. In addition to improved air quality onboard aircraft, an improvement in fuel economy can be realized from removing VOCs via the proposed methodology. Aircraft engines are not just used to propel the plane. Because engines have a source of compressed air for fuel combustion, this is a convenient source for providing compressed air to the cabin. Thus, air is bled from the engines upstream of the combustion chamber to supply the cabin air conditioning system. This bleed air, which is not filtered, may become contaminated with hydraulic oils prior to reaching the cabin. Additionally, since taking this bleed air from the engine reduces the engine’s thrust capacity, it results in lower fuel efficiency.

Some aircraft and engine manufacturers reduce the bleed air requirement by recirculating 50% of the cabin air, which results in an annual savings of about $60,000 per aircraft (95). Recirculated air is typically filtered. The American Society of Heating, Refrigerating and Air-Conditioning Engineers (ASHRAE) requires the use of HEPA

filters for recirculated air (96). HEPA filters will remove 99.97% of 0.3 μm (or larger) particles, which includes some bacteria and viruses. Additionally, sorbent filters (e.g., activated carbon) are sometimes used for VOC and odor control. Because of their typically low adsorption capacity, these filters become ineffective quite rapidly, thus needing regular replacement even before manufacturer-defined intervals (i.e., they reach 100% capacity at five to six months, and become ineffective before then). Better purification methodologies for recirculated air will reduce the need for bleed air, improving fuel economy even further. Technologies also capable of removing potential pollutants from engine bleed air would further increase air quality and reduce the concerns of aerotoxic syndrome.

Experimental

Adsorption

Adsorption experiments were carried out in glass flow-through reactors with the setups shown in Figures A-1 and A-2. Figure A-1 shows the experimental setup for toluene adsorption runs. Figure A-2 shows the experimental setup for ethanol adsorption runs.

The operation of both setups was similar. The contaminant-laden air was mixed in-line with air from a compressed cylinder to achieve the desired contaminant concentration. A bypass allowed for influent samples to be collected. The air then passed through the reactor, where the contaminants were adsorbed onto the STC material, after which effluent samples were collected. Toluene was analyzed via GC/MS with sample collection using a syringe with compound-specific fiber. Ethanol was analyzed via GC/FID with sample collection using NCASI's Chilled Impinger Method (97).

The following parameters were varied:

- STC particle size
- Contact time
- Face velocity
- Influent VOC concentration
- Regeneration method
- Ratio of adsorption duration to regeneration duration

For adsorption studies, STC with a 30 Å pore size and 4% TiO_2 loading were packed in a glass reactor. Contact time was varied by varying the volume of STC added to the reactor. The use of reactors with different cross sectional areas resulted in variation in face velocity.

Regeneration

The STC material was regenerated by passing sweep air through the reactor while irradiating with 254 nm UV. The experimental setup can be seen in Figure A-3. Regeneration times between 30 minutes and 2 hours were investigated.

Results

Adsorption Studies

An experiment was run with 0.25 ppm_v toluene, using 0.6 mm by 1.4 mm STC and a 0.1 s contact time at a 72 ft/min face velocity. As Figure A-4 indicates, toluene removal was greater than 81% throughout the 20-hour adsorption period, with greater than 94% removal for at least 18 hours. In conversations with members of the airline industry it was determined that greater than 50% removal for 20 hours was the goal for long haul flights. Typical VOC concentrations in aircraft cabins range from 0.25 to 0.7 ppm_v, with ethanol being the most concentrated VOC, which was how the influent VOC concentrations were chosen.

The expected face velocity for a full-scale system for this application, based on air-flow rate and cross-sectional area of currently used carbon filters, is 200 ft/min. Thus the impact of increasing the face velocity to 176 ft/min (as close to 200 ft/min as possible based on bench-scale reactor dimensions) was studied and results are plotted in Figure A-5. The influent toluene concentration was 1 ppm_v. Removal was greater than 93% for over eight hours and greater than 70% for 20 hours.

Regeneration of STC

Figure A-6 shows the results of 4-hour adsorption of toluene with an influent concentration of 0.75 ppm_v, followed by 1-hour regeneration with 254 nm UV and vented room temperature sweep air, followed by post-regeneration 4-hour adsorption of 0.75 ppm_v toluene. Adsorption performance was very similar between regenerated and "virgin" (i.e., unused) pellets. The final data point with "virgin" pellets cannot be seen in the graph because it is identical to that with regenerated pellets (i.e., 97.1%).

Ethanol is the most predominant organic pollutant in aircraft cabin air, particularly during food and beverage service. It was expected that if high removal of toluene were obtained during this study, high removal of ethanol would also be obtained. In order to verify this, an experiment was carried out consisting of 20-hour adsorption of 1 ppm_v ethanol, followed by 2-hour regeneration with 254 nm UV plus vented room temperature sweep air, followed by 20-hour post-regeneration adsorption of 1 ppm_v ethanol. Results, which are summarized in Figure A-7, indicate that ethanol adsorption with virgin and regenerated pellets was greater than 93% for 20 hours. Additionally, there was only a slight deterioration in performance when comparing virgin and regenerated pellets.

Because a slight deterioration in performance was observed in several of the regeneration experiments with toluene, an experiment was carried out consisting of multiple cycles of adsorption followed by regeneration with 254 nm UV plus vented room temperature sweep air. A concentration of 0.34 ppm_v toluene was used, with each adsorption cycle lasting two hours and each regeneration cycle lasting 30 minutes, plus a final regeneration period lasting four hours.

As Figure A-8 indicates, there was some deterioration in performance as additional regeneration cycles progressed, although a final 4-hour regeneration restored most of the STC's adsorption capacity. It should be noted that toluene is more challenging to adsorb and oxidize than other VOCs that are more predominant in aircraft cabins. Thus, although it is apparent that there may be some accumulation of toluene remaining on the STC at the end of each regeneration cycle, the more easily destructible VOCs, such as ethanol, which is abundant in aircraft cabins, were expected to be fully oxidized to CO_2 and water. Figure A-8, along with the superior data for ethanol (Figure A-7), which makes up about 85% of total VOC concentration in aircraft cabins, lead one to expect the STC technology to retain its high performance even after multiple regenerations in a real world scenario.

Summary

The effectiveness of the STC technology for removal of VOCs for application in aircraft cabin air purification was successfully demonstrated. It was determined that the STC can effectively remove toluene and ethanol via adsorption alone. Regeneration with 254 nm UV plus sweep air was proven effective for average flight lengths (i.e., 4 hours). When using ethanol as the target pollutant, regeneration with 254 nm UV plus

sweep air was proven effective for long haul flights, which indicates it would also be effective for shorter flights.

Commercial systems employing photocatalysis for the removal of gas-phase contaminants have limitations (88). Typical photocatalytic systems employ a thin film of titania (98, 99), which can be easily damaged and results in poor mass transfer of the pollutants to the catalyst. In addition, photocatalytic systems typically require constant UV irradiation, and may lead to incomplete oxidation of organic compounds, which is a major concern for aircraft cabin air purification. The STC technology overcomes these limitations of typical PCO systems. Not only is the catalyst trapped within a silica matrix rather than coated, but the high surface area adsorbent also allows for the preferred operation of adsorption during flight and regeneration between flights. This mode of operation would not only achieve high levels of contaminant removal, but would also eliminate the possibility of releasing toxic intermediate oxidation by-products into the air during flight.

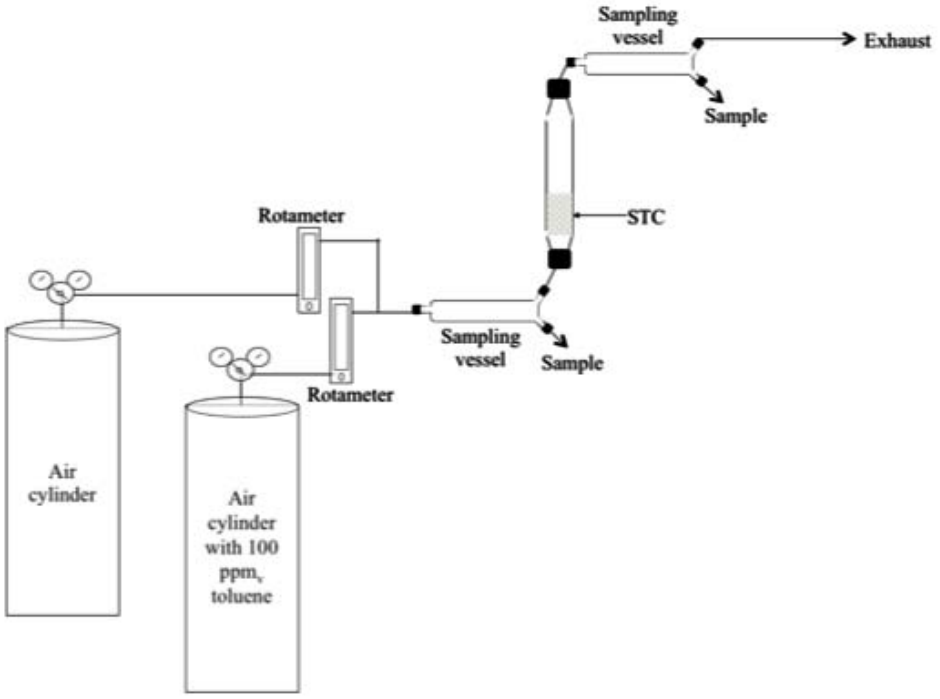

Figure A-1. Experimental setup for toluene adsorption.

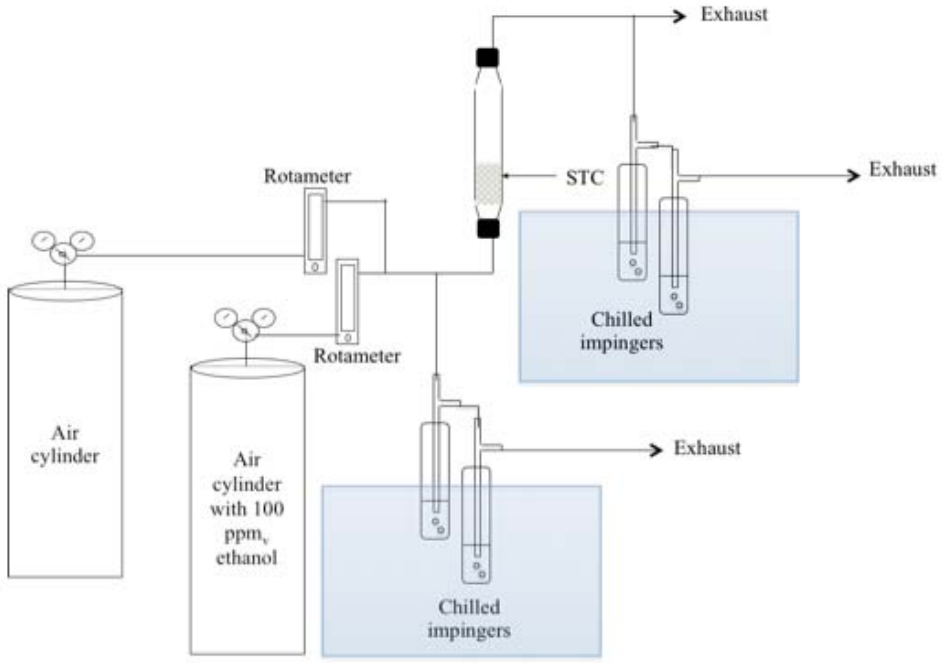

Figure A-2. Experimental setup for ethanol adsorption.

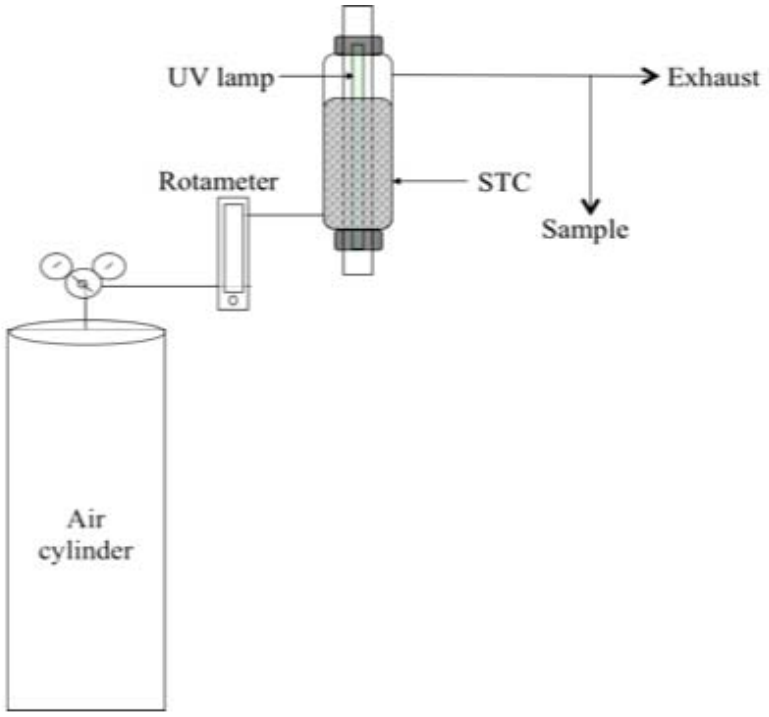

Figure A-3. Experimental setup for regeneration.

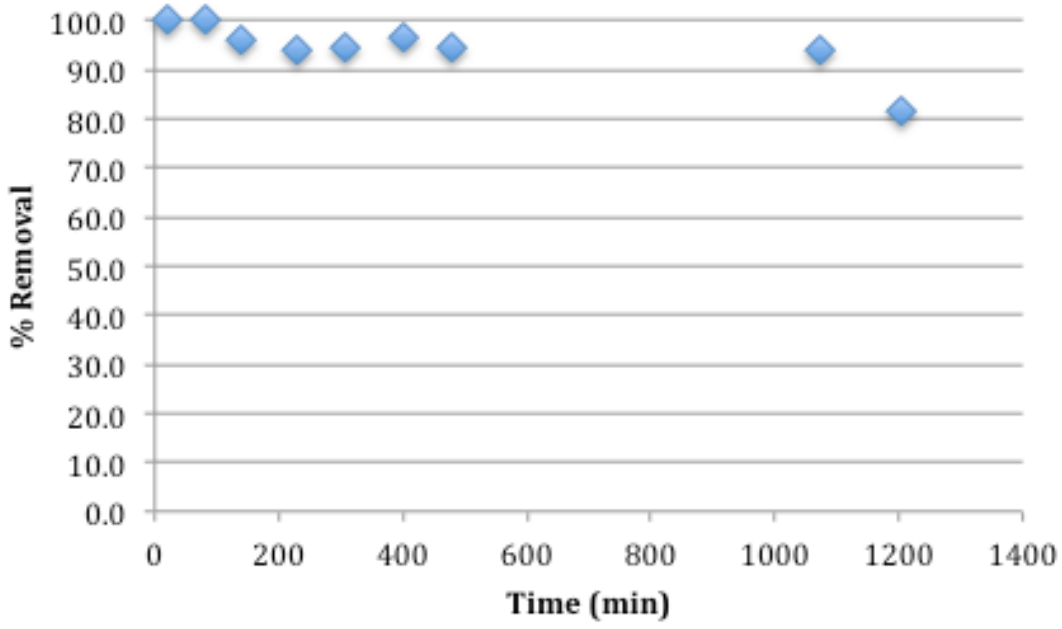

Figure A-4. Toluene adsorption at 72 ft/min face velocity.

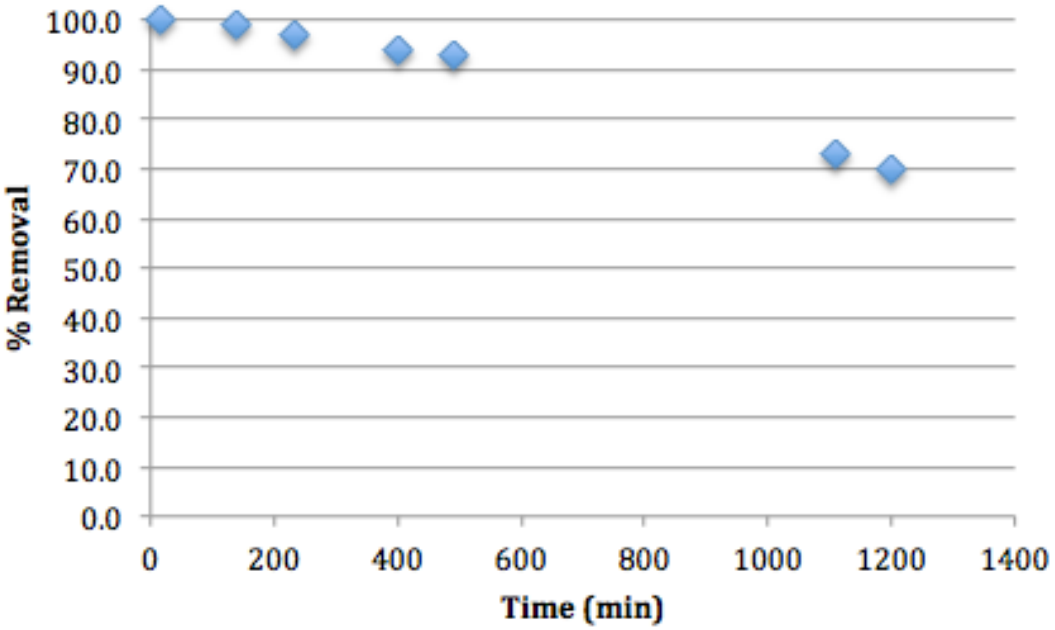

Figure A-5. Toluene adsorption at 176 ft/min face velocity.

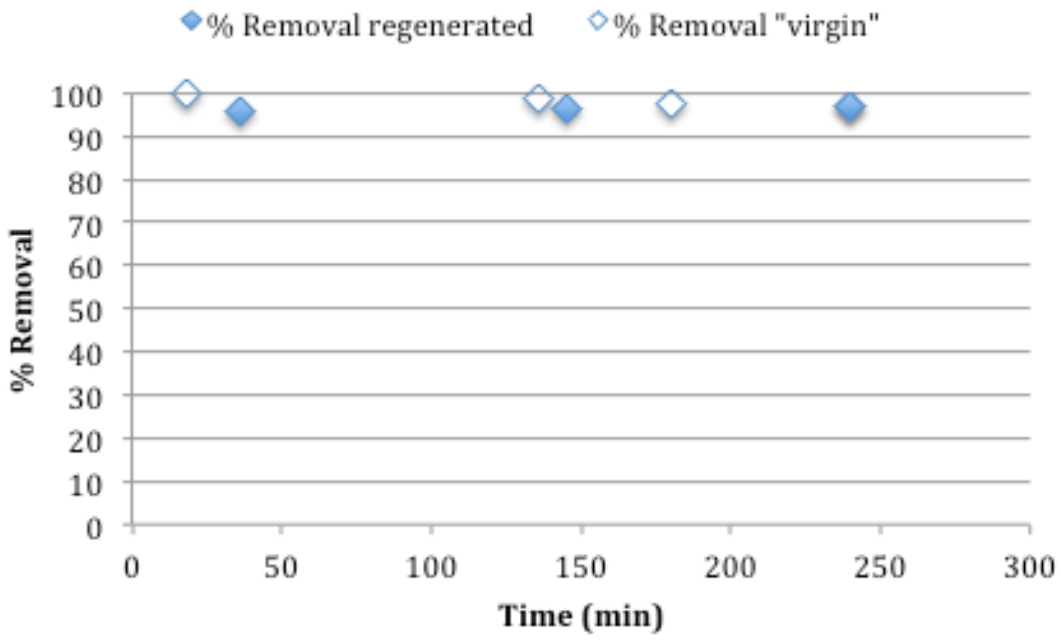

Figure A-6. Toluene adsorption by virgin and regenerated STC pellets. Note that the virgin and regenerated pellets remove the same percentage of toluene at the last data point.

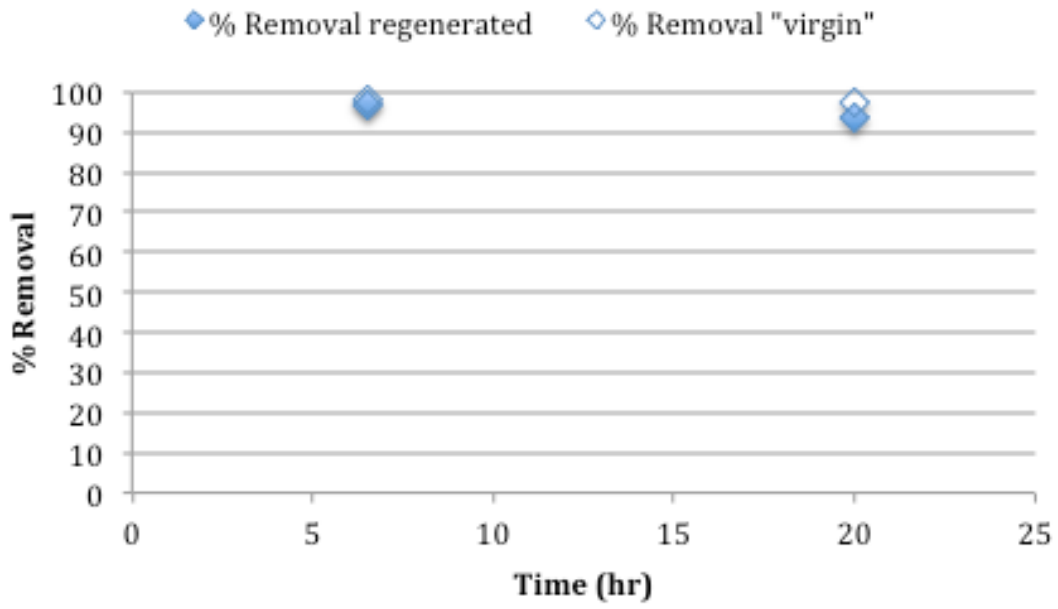

Figure A-7. Ethanol removal before and after regeneration with sweep air.

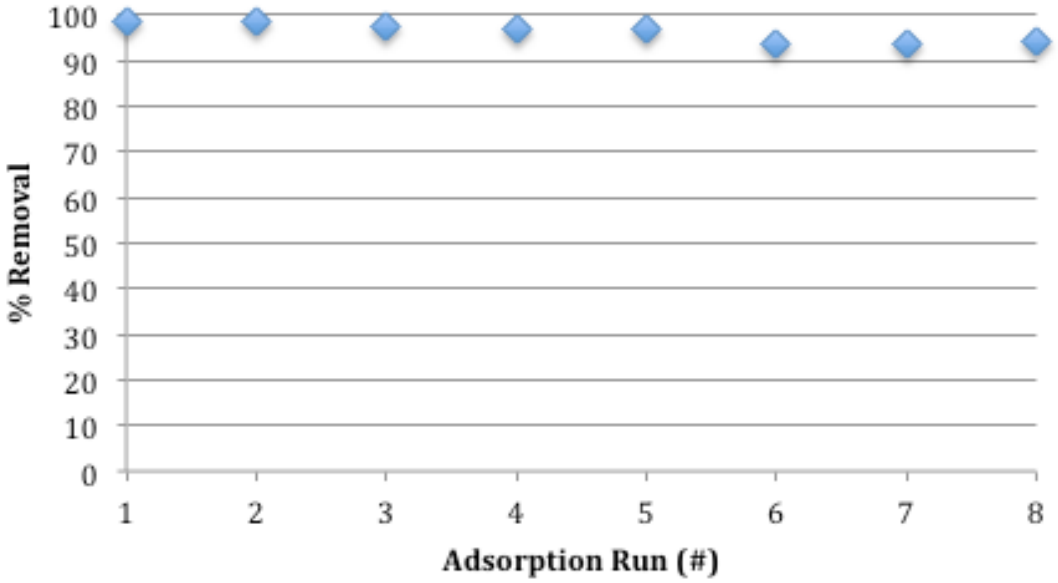

Figure A-8. Toluene removal after several regenerations with sweep air.

LIST OF REFERENCES

(1) Hankey, R.; Cassar, C.; Peterson, R.; Harris-Russel, C.; Knaub Jr., J. *Electric Power Monthly*. 2011, March. Washington, D.C.: U.S. Energy Information Administration.

(2) Pai, P.; Niemi, D.; Powers, B. A North American inventory of anthropogenic mercury emissions .*Fuel Processing Technology.* **2000,** 65-66, 101-115.

(3) Pacyna, E. G.; Pacyna, J. M.; Steenhuisen, F.; Wilson, S. Global anthropogenic mercury emission inventory for 2000. *Atmospheric Environment.* **2006,** 40, 4048 - 4063.

(4) USEPA Nitrogen Dioxide Primary Standards. 2011. http://www.epa.gov/ttn/naaqs/standards/nox/s_nox_index.html.

(5) USEPA Sulfur Dioxide Primary National Ambient Air Quality Standards. 2011. http://www.epa.gov/ttn/naaqs/standards/so2/s_so2_index.html

(6) S.1630 - Clean Air Act Ammendments of 1990. Washington, D.C. 1990.

(7) Study of Hazardous Air Pollutant Emisions From Electric Utility Steam Generating Units - Final Report to Congress. Washington, D.C.: U.S. Government Printing Office. 1998.

(8) Keating, M. H.; Beauregard, D.; Benjey, W. G.; Driver, L.; Maxwell, W. H.; Peters, W. D. Mercury study report to congress Volume 2: An inventory of anthropogenic mercury emissions in the United States.1997. *EPA-452/R-97-004*.

(9) Wiatrowski, K. EPA tightening mercury emissions rules. 30 May, 2011. *http://www2.Tbo.com/news/news/2011/may/30/menewso6-epa-tightening-mercury-emissions-rules-ar-233662/*

(10) Power, S. EPA rule targets mercury pollution. March 17, 2011. http://online.wsj.com/article/SB10001424052748703899704576204583816132832.html

(11) Slemr, F.; Schuster, G.; Seiler, W. Distribution, speciation, and budget of atmospheric mercury. *Journal of atmospheric chemistry.* **1985,** 3, 407-434.

(12) Lindqvist, O.; Rodhe, H. Atmospheric mercury - a review. *Tellus B.* **1985,** 37, 136-159.

(13) Wang, Q.; Shen, W.; Ma, Z. Estimation of Mercury Emission from Coal Combustion in China. *Environmental Science & Technology.* **2000,** 34, 2711-2713.

(14) *Managing Coal Combustion Residues in Mines.* Washington, D.C., The National Academics Press, 2006.

(15) Scala, F. Simulation of mercury capture by activated carbon injection in incinerator flue gas. In-duct removal. *Environmental Science & Technology.* **2001,** 35, 4367-4372.

(16) Jones, A. P.; Hoffmann, J. W.; Smith, D. N.; Feeley, T. J.; Murphy, J. T. DOE/NETL's phase II mercury control technology field testing program: Preliminary economic analysis of activated carbon injection. *Environmental Science & Technology.* **2007,** 41, 1365-1371.

(17) Huggins, F. E.; Yap, N.; Huffman, G. P.; Senior, C. L. XAFS characterization of mercury captured from combustion gases on sorbents at low temperatures. *Fuel Processing Technology.* **2003,** 82, 167-196.

(18) Mercury Study Report to Congress Volume 5: Health Effects of Mercury and Mercury Compounds. Mercury study report to congress volume 5: Health effects of mercury and mercury compounds.1997.

(19) Pitoniak, E. Evaluation of nanostructured silica-titania composites in an adsorption/photocatalytic oxidation system for elemental mercury vapor control. Master of Engineering Thesis, University of Florida. 2004

(20) Li, Y.; Murphy, P.; Wu, C. Y. Removal of elemental mercury from simulated coal-combustion flue gas using a SiO_2-TiO_2 nanocomposite. *Fuel Processing Technology.* **2008,** 89, 567-573.

(21) Robertson, P.; Bahnemann, D.; Robertson, J.; Wood, F. Photocatalytic detoxification of water and air. *Environmental Photochemistry.* **2005,** 2, 367-423.

(22) Hoffmann, M. R.; Martin, S. T.; Choi, W.; Bahnemann, D. W.Environmental applications of semiconductor photocatalysis. *Chemical Reviews.* **1995,** 95, 69-96.

(23) Al-Ekabi, H.; Serpone, N. Kinetic Studies In Heterogeneous Photocatalysis. Photocatalytic Degradation of Chlorinated Phenols In Aerated Aqueous Solutions Over TiO_2 Supported On A Glass Matrix. *Journal of Physical Chemistry.* **1988,** 92, 5726-5731.

(24) Wu, C. Y.; Lee, T. G.; Tyree, G.; Arar, E.; Biswas, P. Capture of Mercury in Combustion Systems by In Situ--Generated Titania Particles with UV Irradiation. *Environmental Engineering Science.* **1998,** 15, 137-148.

(25) Pitoniak, E.; Wu, C. Y.; Londeree, D.; Mazyck, D.; Bonzongo, J. C.; Powers, K.; Sigmund, W. Nanostructured silica-gel doped with TiO_2 for mercury vapor control. *Journal of Nanoparticle Research.* **2003,** 5, 281-292.

(26) Hall, B.; Schager, P.; Lindqvist, O. Chemical reactions of mercury in combustion flue-gases. *Water and Soil Pollution.* **1991,** 56, 3-14.

(27) Sliger, R. N.; Kramlich, J. C.; Marinov, N. M. Towards the development of a chemical kinetic model for the homogeneous oxidation of mercury by chlorine species. *Fuel Processing Technology.* **2000,** 65-66, 423-438.

(28) Lindberg, S. E.; Stratton, W. J. Atmospheric mercury speciation: Concentrations and behavior of reactive gaseous mercury in ambient air. *Environmental Science & Technology.* **1998,** 32, 49-57.

(29) Cao, Y.; Chen, B.; Wu, J.; Cui, H.; Smith, J.; Chen, C.; Chu, P.; Pan, W. Study of Mercury Oxidation by a Selective Catalytic Reduction Catalyst in a Pilot-Scale Slipstream Reactor at a Utility Boiler Burning Bituminous Coal. *Energy & Fuels.* **2007,** 21, 145-156.

(30) Galbreath, K. C.; Zygarlicke, C. J. Mercury speciation in coal combustion and gasification flue gases. *Environmental Science & Technology.* **1996,** 30, 2421-2426.

(31) Kilgroe, J. D.;Sedman, C. B.;Srivastava, R. K.; Ryan, J. V.; Lee, C. W.; Thornloe, S. A. Control of Hg emissions from coal-fired electric utility boilers: Interim report. 1997. EPA-600/R-01-109.

(32) Lee, S. J.; Seo, Y.; Jang, H.; Park, K.; Baek, J.; An, H.; Song, K. Speciation and mass distribution of mercury in a bituminous coal-fired power plant. *Atmospheric Environment.* **2006,** 40, 2215-2224.

(33) Niksa, S.; Fujiwara, N. Predicting extents of mercury oxidation in coal-derived flue gases. *Journal of the Air and Waste Management Association.* **2005,** 55, 930-939.

(34) Clever, H. L.; Johnson, S. A.; Derrick, M. E. The solubility of mercury and some sparingly soluble mercury salts in water and aqueous electrolyte solutions. *Journal of Physical and Chemical Reference Data.* **1985,** 14, 631.

(35) Edwards, J. R.; Srivastava, R. K.; Kilgroe, J. D. A study of gas-phase mercury speciation using detailed chemical kinetics. *Journal of the Air & Waste Management Association.* **2001,** 51, 869-877.

(36) Fujiwara, N.; Fujita, Y.; Tomura, K.; Moritomi, H.; Tuji, T.; Takasu, S.; Niksa, S. Mercury transformations in the exhausts from lab-scale coal flames. *Fuel.* **2002,** 81, 2045-2052.

(37) Meij, R.; Vredenbregt, L. H. J.; Winkel, H. T. The fate and behavior of mercury in coal-fired power plants. *Journal of the Air & Waste Management Association.* **2002,** 52, 912-917.

(38) Niksa, S.; Fujiwara, N. A predictive mechanism for mercury oxidation on selective catalytic reduction catalysts under coal-derived flue gas. *Journal of the Air and Waste Management Association.* **2005,** 55, 1866-1875.

(39) Sable, S. P.; de Jong, W.; Spliethoff, H. Combined Homo- and Heterogeneous Model for Mercury Speciation in Pulverized Fuel Combustion Flue Gases. *Energy & Fuels.* **2008,** 22, 321-330.

(40) Senior, C. L.; Sarofim, A. F.; Zeng, T. F.; Helble, J. J.; Mamani-Paco, R. Gas-phase transformations of mercury in coal-fired power plants. *Fuel Processing Technology.* **2000,** 63, 197-213.

(41) Pavlish, J. H.; Sondreal, E. A.; Mann, M. D.; Olson, E. S.; Galbreath, K. C.; Laudal, D. L.; Benson, S. A Status review of mercury control options for coal-fired power plants. *Fuel Processing Technology.* **2003,** 82, 89-165.

(42) Ghorishi, S. B.; Sedman, C. B. Low concentration mercury sorption mechanisms and control by calcium-based sorbents: Application in coal-fired processes. *Journal of the Air & Waste Management Association.* **1998,** 48, 1191-1198.

(43) Zhao, Y. X.; Mann, M. D.; Olson, E. S.; Pavlish, J. H.; Dunham, G. E. Effects of sulfur dioxide and nitric oxide on mercury oxidation and reduction under homogeneous conditions. *Journal of the Air and Waste Management Association.* **2006,** 56, 628-635.

(44) Heebink, L. V.; Hassett, D. J. Release of mercury vapor from coal combustion ash. *Journsl of the Air and Waste Management Associstion.* **2002,** 52, 927-930.

(45) Hrdlicka, J. A.; Seames, W. S.; Mann, M. D.; Muggli, D. S.; Horabik, C. A. Mercury Oxidation in Flue Gas Using Gold and Palladium Catalysts on Fabric Filters. *Environmental Science & Technology.* **2008,** 42, 6677-6682.

(46) Presto, A. A.; Granite, E. J. Noble Metal Catalysts for Mercury Oxidation in Utility Flue Gas: Gold, Palladium and Platinum Formulations. *Platinum Metals Review.* **2008,** 52, 144-154.

(47) Jadhav, R .A.; Meyer, H. S.; Winecki, S.; Breault, R. W. Evaluation of nanocrystalline sorbents for mercury removal from coal gasifier fuel gas. *In The 2005 Annual Meeting. AIChE..* Cincinnati, OH. 2005.

(48) Benson, S. A.; Laumb, J. D.; Crocker, C. R.; Pavlish, J. H. SCR catalyst performance in flue gases derived from subbituminous and lignite coals. *Fuel Processing Technology.* **2005,** 86, 577-613.

(49) Cao, Y.; Duan, Y.; Kellie, S.; Li, L.; Xu, W.; Riley, J. T.; Pan, W. P.; Chu, P.; Mehta, A. K.; Carty, R. Impact of coal chlorine on mercury speciation and emission from a 100-MW utility boiler with cold-side electrostatic precipitators and low-NOx burners. *Energy and Fuels.* **2005,** 19, 842-854.

(50) Stokke, J. M.; Mazyck, D. W.; Wu, C. Y.; Sheahan, R. Photocatalytic oxidation of methanol using silica-titania composites in a packed-bed reactor. *Environmental Progress.* **2006,** 25, 312-318.

(51) Stokke, J. M.; Mazyck, D. W. Development of a regenerable system employing silica-titania composites for the recovery of mercury from end-box exhaust at a chlor-alkali facility. *Journal of the Air and Waste Management Association.* **2008,** 58, 530-537.

(52) Gruss, A. F.; Casasús, A. I.; Mazyck, D. W. VOC removal by novel regenerable silica-titania sorbent and photocatalytic technology. *In Proceedings from the 39th International Conference on Environmental Systems.* Savannah, Georgia. July, 2009.

(53) Londerée, D. J. Silica-titania composites for water treatment. Master of Engineering Thesis, University of Florida. 2002.

(54) Powers, K. W. The development and characterization of sol-gel substrates for chemical and optical applications. PhD Dissertation, University of Florida. 1998.

(55) Li, Y.; Lee, S. R.; Wu, C. Y. UV-Absorption-Based Measurements of Ozone and Mercury: An Investigation on Their Mutual Interferences. *Aerosol and Air Quality Research.* **2006,** 6, 418-429.

(56) Li, Y.; Wu, C. Y. Kinetic study for photocatalytic oxidation of elemental mercury on a SiO_2-TiO_2 nanocomposite. *Environmental Engineering Science.* **2007,** 24, 3-12.

(57) Dickinson, R. G.; Sherrill, M. S. Formation of ozone by optically excited mercury vapor. *Proceedings of the National Academy of Sciences of the United States of America.* **1926,** 12, 175-178.

(58) Granite, E. J.; Pennline, H. W. Photochemical removal of mercury from flue gas. *Industrial & Engineering Chemistry Research.* **2002,** 41, 5470-5476.

(59) Jia, L.; Dureau, R.; Ko, V.; Anthony, E. J. Oxidation of Mercury under Ultraviolet (UV) Irradiation. *Energy & Fuels.* **2010,** 24, 4351-4356.

(60) Lee, T. G.; Biswas, P.; Hedrick, E. Overall kinetics of heterogeneous elemental mercury reactions on TiO_2 sorbent particles with UV irradiation. *Industrial & Engineering Chemistry Research.* **2004,** 43, 1411-1417.

(61) Perry, R. H.; Green, D. W.; Maloney, J. O. *Perry's Chemical Engineers' Handbook* .New York, McGraw-Hill, 1984.

(62) Lide, D. R. *CRC Handbook of Chemistry and Physics, 2000-2001: A Ready-Reference Book of Chemical and Physical Data.* CRC press, 2000.

(63) Dasent, W. E. *Inorganic Energetics: An introduction.* New York, Cambridge University Press, 1982.

(64) Cauch, B.; Silcox, G. D.; Lighty, J. S.; Wendt, J. O. L.; Fry, A.; Senior, C. L. Confounding Effects of Aqueous-Phase Impinger Chemistry on Apparent Oxidation of Mercury in Flue Gases. *Environ Sci. Technol.* **2008,** .

(65) Byun, Y.; Ko, K. B.; Cho, M.; Namkung, W.; Shin, D. N.; Lee, J. W.; Koh, D. J.; Kim, K. T. Oxidation of elemental mercury using atmospheric pressure non-thermal plasma. *Chemosphere.* **2008,** 72, 652-658.

(66) Ko, K. B.; Byun, Y.; Cho, M.; Namkung, W.; Hamilton, I. P.; Shin, D. N.; Koh, D. J.; Kim, K. T. Pulsed corona discharge for oxidation of gaseous elemental mercury. *Applied Physics Letters.* **2008,** 92, 251503-251503.

(67) Hall, B. The gas-phase oxidation of elemental mercury by ozone. *Water, Air, & Soil Pollution.* **1995,** 80, 301-315.

(68) Fujishima, A.; Rao, T. N.; Tryk, D. A. Titanium dioxide photocatalysis. *Journal of Photochemistry and Photobiology C: Photochemistry Reviews.* **2000,** 1, 1-21.

(69) Lukes, P.; Appleton, A. T.; Locke, B. R. Hydrogen peroxide and ozone formation in hybrid gas-liquid electrical discharge reactors. *IEEE Transactions on Industry Applications.* **2004,** 40, 60-67.

(70) Caren, R. P.; Ekchian, J. A. Method for Using Hydroxyl Radical to Reduce Pollutants in the Exhaust Gases from the Combustion of a Fuel. U.S. Patent 5,863,413, Jan 26, 1999.

(71) Zhang, H.; Lindberg, S. E. Sunlight and iron (III)-induced photochemical production of dissolved gaseous mercury in freshwater. *Environmental Science & Technology.* **2001,** 35, 928-935.

(72) Grosjean, D.; Harrison, J. Response of chemiluminescence NOx analyzers and ultraviolet ozone analyzers to organic air pollutants. *Environmental Science & Technology.* **1985,** 19, 862-865.

(73) Bader, H.; Sturzenegger, V.; Hoigne, J. Photometric method for the determination of low concentrations of hydrogen peroxide by the peroxidase catalyzed oxidation of N, N-diethyl-p-phenylenediamine (DPD). *Water Res.* **1988,** 22, 1109-1115.

(74) Jeon, S. H.; Eom, Y.; Lee, T. G. Photocatalytic oxidation of gas-phase elemental mercury by nanotitanosilicate fibers. *Chemosphere.* **2008,** 71, 969-974.

(75) Li, J.; Yan, N.; Qu, Z.; Qiao, S.; Yang, S.; Guo, Y.; Liu, P.; Jia, J. Catalytic Oxidation of Elemental Mercury over the Modified Catalyst Mn/Î±-Al2O3 at Lower Temperatures. *Environmental Science & Technology.* **2010,** 44, 426-431.

(76) Norton, G. A.; Yang, H.; Brown, R. C.; Laudal, D. L.; Dunham, G. E.; Erjavec, J. Heterogeneous oxidation of mercury in simulated post combustion conditions. *Fuel.* **2003,** 82, 107-116.

(77) Takahashi, K.; Kasahara, M.; Itoh, M. A kinetic model of sulfuric acid aerosol formation from photochemical oxidation of sulfur dioxide vapor. *Journal of Aerosol Science.* **1975,** 6, 45-55.

(78) Byun, Y.; Cho, M.; Namkung, W.; Lee, K.; Koh, D. J.; Shin, D. N. Insight into the Unique Oxidation Chemistry of Elemental Mercury by Chlorine-Containing Species: Experiment and Simulation. *Environmental Science & Technology.* **2010,** 44, 1624-1629.

(79) Ochiai, R.; Uddin, M. A.; Sasaoka, E.; Wu, S. Effects of HCl and SO_2 Concentration on Mercury Removal by Activated Carbon Sorbents in Coal-Derived Flue Gas. *Energy & Fuels.* **2009,** 23, 4734-4739.

(80) Pitoniak, E.; Wu, C. Y.; Mazyck, D. W.; Powers, K. W.; Sigmund, W. Adsorption enhancement mechanisms of silica-titania nanocomposites for elemental mercury vapor removal. *Environmental Science & Technology.* **2005,** 39, 1269-1274.

(81) McDowell, M. A.; Dillon, C. F.; Osterloh, J.; Bolger, P. M.; Pellizzari, E.; Fernando, R.; de Oca, R. M.; Schober, S. E.; Sinks, T.; Jones, R. L.; Mahaffey, K. R. Hair mercury levels in US children and women of childbearing age: Reference range data from NHANES 1999-2000. *Environmental Health Perspectives.* **2004,** 112, 1165-1171.

(82) Cheuk, D. K. L.; Wong, V. Attention-deficit hyperactivity disorder and blood mercury level: a case-control study in Chinese children. *Neuropediatrics.* **2006,** 37, 234-240.

(83) USDOE Mercury Emission Control R&D. 2005. http://www.fossil.energy.gov/programs/powersystems/pollutioncontrols/overview_mercurycontrols.html

(84) CATM Annual Report: Toxic Metal Transformation in Fossil Fuel Combustion Systems. 2008. www.undeerc.org/catm/pdf/area1/2008ToxicMetalTransformations.pdf

(85) Mercury Control Plan for Sherco Units 1 & 2 Pursuant to the Minnesota Mercury Emission Reduction Act of 2006. 2009.

(86) Li, Y.; Daukoru, M.; Suriyawong, A.; Biswas, P. Mercury Emissions Control in Coal Combustion Systems Using Potassium Iodide: Bench-Scale and Pilot-Scale Studies. *Energy & Fuels.* **2009,** 23, 236-243.

(87) Winder, C.; Balouet, J. C. The toxicity of commercial jet oils. *Environmental Research.* **2002,** 89, 146-164.

(88) Devilliers, D. Semiconductor photocatalysis: still an active research area despite barriers to commercialization. *Energeia.* **2006,** 17, 1-3.

(89) Stokke, J. M.; Mazyck, D. W. Effect of Catalyst Support on the Photocatalytic Destruction of VOCs in a Packed-Bed Reactor. **2007,** .

(90) Stokke, J. M.; Mazyck, D. W. Photocatalytic Degradation of Methanol Using Silica-Titania Composite Pellets: Effect of Pore Size on Mass Transfer and Reaction Kinetics. *Environmental Science & Technology.* **2008,** 42, 3808-3813.

(91) Termaath, C.; Holmes, F.; Drwiega, J.; Londeree, D.; Mazyck, D.; Powers, K.; Chadik, P.; Wu, C. Comparison of nanoparticles for the photocatalytic destruction of organic pollutants for water recovery. *In 33rd International Conference on Environmental Systems 2003, 2003-01-2334, Vancouver, BC..* 2003.

(92) Holmes, F. R.; Chadik, P. A.; Mazyck, D. W.; Wu, C. Y.; Garton, M. J.; Powers, K. W.; Londeree, D. J. Photocatalytic oxidation of selected organic contaminants in a continuous flow reactor packed with titania-doped silica. *In 34th International Conference on Environmental Systems. Colorado Springs, CO, USA.* 2004.

(93) Ludwig, C. Y.; Byrne, H. E.; Stokke, J. M.; Chadik, P. A.; Mazyck, D. W. Performance of Silica-Titania Carbon Composites for Photocatalytic Degradation of Gray Water. *Journal of Environmental Engineering.* **2011,** 137, 38.

(94) Garton, M. J.; Chadik, P. A.; Mazyck, D. W. *Photocatalytic oxidation of selected organic contaminants and inactivation of microorganisms in a continuous flow reactor packed with titania-doped silica*. Master of Engineering Thesis. University of Florida. 2005.

(95) Michaelis, S.; Loraine, T. Aircraft Cabin Air Filtration and Related Technologies: Requirements, Present Practice and Prospects. *Air Quality in Airplane Cabins and Similar Enclosed Spaces.* **2005,** 267-289.

(96) ASHRAE STANDARD 161: Air Quality within Commercial Aircraft, American Society of Heating, Refrigerating and Air-Conditioning Engineers. 2007.

(97) NCASI Chilled Impinger Test Method for Use on Pulp Mill Sources to Quantify Methanol Emissions.National Council for Air and Stream Improvement. Method CI/GS/PULP-94.03. February 2005.

(98) Ginestet, A.; Pugnet, D.; Rowley, J.; Bull, K.; Yeomans, H. Development of a new photocatalytic oxidation air filter for aircraft cabin. *Indoor Air.* **2005,** 15, 326-334.

(99) Sun, Y.; Fang, L.; Wyon, D. P.; Wisthaler, A.; Lagercrantz, L.; Strøm-Tejsen, P. Experimental research on photocatalytic oxidation air purification technology applied to aircraft cabins. *Building and Environment.* **2008,** 43, 258-268.

BIOGRAPHICAL SKETCH

Alexander Ferdinand Gruss was born in Filderstadt, Germany in September of 1982. He attended the Swiss Federal Institute of Technology from October 2002 until October 2004, receiving the equivalent of an associate's degree in Civil Engineering. After transferring to the University of Florida in 2005, he graduated Magna cum Laude with a B.S. in Civil Engineering in May of 2007. During his last semester, he began working on air-phase mercury removal using a novel photocatalytic silica-titania composite material. He continued this work in graduate school under the guidance of Dr. David Mazyck and received his Ph.D. from the University of Florida in the summer of 2011.